



HR3DHG version 1: modelling the spatio-temporal dynamics of mercury in the Augusta Bay (southern Italy)

Giovanni Denaro¹, Daniela Salvagio Manta², Alessandro Borri³, Maria Bonsignore², Davide Valenti^{1,4}, Enza Quinci², Andrea Cucco⁵, Bernardo Spagnolo^{4,6,7}, Mario Sprovieri², and Andrea De Gaetano³

¹CNR-IRIB, Consiglio Nazionale delle Ricerche Istituto per la Ricerca e l'Innovazione Biomedica, Via Ugo La Malfa 153, I-90146 Palermo, Italy

²CNR-IAS, Consiglio Nazionale delle Ricerche Istituto per lo studio degli impatti Antropici e Sostenibilità in ambiente marino, U.O.S di Capo Granitola, Via del Faro 3, I-91020 Campobello di Mazara (TP), Italy

³CNR-IASI Biomathematics Laboratory, Consiglio Nazionale delle Ricerche Istituto di Analisi dei Sistemi ed Informatica "A. Ruberti", Via dei Taurini 19, I-00185 Rome, Italy

⁴Dipartimento di Fisica e Chimica "Emilio Segrè", Università di Palermo, Group of Interdisciplinary Theoretical Physics and CNISM, Unità di Palermo, Viale delle Scienze, Ed. 18, I-90128 Palermo, Italy

⁵CNR-IAS, Consiglio Nazionale delle Ricerche Istituto per lo studio degli impatti Antropici e Sostenibilità in ambiente marino, U.O.S. di Oristano, località Sa Mardini, I-09072 Torregrande (OR), Italy

⁶Radiophysics Department, National Research Lobachevsky State University of Nizhni Novgorod, 23 Gagarin Avenue, Nizhni Novgorod 603950, Russia

⁷Istituto Nazionale di Fisica Nucleare, Sezione di Catania, Via S. Sofia 64, I-90123 Catania, Italy

Correspondence: Alessandro Borri (alessandro.borri@iasi.cnr.it)

Abstract. The biogeochemical dynamics of Hg , and specifically of its three species Hg^0 , Hg^{II} , and $MeHg$ (elemental, inorganic, and organic, respectively) in the marine coastal area of Augusta Bay (southern Italy) have been explored by the high resolution 3D Hg (HR3DHG) model, namely an advection-diffusion-reaction model for the dissolved mercury in the seawater compartment coupled with i) a diffusion-reaction model for dissolved mercury in the pore water of sediments and ii) a sorption/de-sorption model for total mercury in the sediments. The spatio-temporal variability of dissolved and total mercury concentration both in seawater ($[Hg_D]$ and $[Hg_T]$) and first layers of bottom sediments ($[Hg_D^{sed}]$ and $[Hg_T^{sed}]$), and the Hg fluxes at the boundaries of the 3D model domain have been theoretically reproduced, showing an excellent agreement with the experimental data, collected in multiple field observations during six different oceanographic cruises. The mass-balance of the different Hg species in seawater has been calculated for the Augusta Harbor, improving previous estimations. The HR3DHG model includes modules that can be implemented for specific and detailed exploration of the effects of climate change on the spatio-temporal distribution of Hg in highly contaminated coastal-marine areas.



1 Introduction

15 The investigation of biogeochemical dynamics of Hg species in the marine environment addresses the need to accurately model sources and pathways of this priority contaminant within and among the different abiotic and biotic compartments of the aquatic ecosystem (Driscoll et al., 2013; Batrakova et al., 2014). Over the last few years some theoretical studies have offered sophisticated tools to reproduce the mass balance and the dynamics of $[Hg]$ in the marine environment by means of biogeochemical models based on interconnected zero dimensional boxes, representing water or sediment compartments:

20 among these is the WASP (Water Analysis Simulation Program) model (Zhang et al., 2014; Melaku Canu et al., 2015; Ciffroy, 2015). Recently (Zhang et al., 2014; Melaku Canu et al., 2015) a WASP-based approach has been adopted to calculate Hg mass balance in the coastal areas of the Marano-Grado lagoon (northern Italy). Similarly, a box-model approach has been adopted by the River MERLIN-Expo model (Ciffroy, 2015), which has been used to reproduce the spatio-temporal distribution of inorganic and organic contaminants in the abiotic compartments of rivers, and to calculate $[Hg]$ mass balance for each of

25 them. Although the River model is able to describe many of the physical and chemical processes involved in freshwater and sediment, corresponding this model specifically targets environments characterized by (i) nearly-homogeneous water bodies and (ii) limited variations in landscape geometry. In general, models based on zero dimensional boxes do not deliver reliable concentration values of contaminants in highly heterogeneous environments. For this reason, in more recent works (Yakushev et al., 2017; Pakhomova et al., 2018) the biochemistry of Hg in aquatic ecosystems has been studied using a 1D advection-

30 reaction-diffusion model: the Bottom RedOx Model (BROM) has been used to reproduce the vertical dynamics of the total dissolved Hg and $MeHg$ in the marine coastal areas of the Etang de Berre lagoon (France) (Pakhomova et al., 2018). However, even the BROM includes some criticalities in the estimation of mercury dynamics. For example, the temporal variations of mercury benthic fluxes, due to reaction and diffusion processes which involve mercury species present in sediments, are not taken into account in the boundary conditions of this model.

35 All these approaches forego the complete representation of the spatial variability by approximating the model domain as a set of interconnected boxes or by detailing only the vertical dynamics of the investigated chemical species. In the present work we report on results obtained using a 3D advection-diffusion-reaction biogeochemical model for three Hg species in seawater (Hg^0 , Hg^{II} , and $MeHg$), coupled with a diffusion-reaction model in sediments and connected pore water. The model, named HR3DHG, has been applied to the investigation of the mercury dynamics in Augusta Bay (southern Italy, see

40 Fig. 1) and specifically in its harbor, a highly polluted coastal site. In this area, a substantial experimental dataset has been collected and improved upon in recent years (Sprovieri et al., 2011; Bagnato et al., 2013; Sprovieri, 2015; Oliveri et al., 2016; Salvagio Manta et al., 2016): oceanographic cruises and data on key physical and chemical parameters from atmosphere, seawater and sediments are used to verify and validate the modules of HR3DHG for reliable and accurate high-resolution investigation of spatio-temporal dynamics of Hg in highly contaminated coastal-marine sites. The HR3DHG model has been

45 designed to predict the biogeochemical behavior of Hg in seawater and sediments, specifically in confined and highly-polluted marine-coastal areas. It offers the opportunity to explore the effects both of sorption/de-sorption dynamics of total mercury (Hg_T^{sed}) in sediments, and of Hg_D^{sed} diffusion dynamics in pore water. The role played by the spatio-temporal behavior of



phytoplankton (La Barbera and Spagnolo, 2002; Fiasconaro et al., 2004; Valenti et al., 2004, 2008; Dutkiewicz et al., 2009; Morozov et al., 2010; Valenti et al., 2012; Denaro et al., 2013a, c, b; Valenti et al., 2015, 2016a, b, c, 2017) and the potential mechanisms responsible for the uptake of Hg within cells (Pickhardt and Fischer, 2007; Radomyski and Ciffroy, 2015; Lee and Fischer, 2017; Williams et al., 2010) are specifically addressed. Seasonal oscillations of key environmental variables (velocity of marine currents, amount of precipitation, elemental and inorganic mercury concentration in atmosphere, etc.) are taken into account. The HR3DHG model offers the possibility to describe the $MeHg$ and Hg^{II} partition between the dissolved phase (both seawater and pore water) and the particulate phase (suspended particulate matter and sediment particles). This module includes a representation of the behavior of Hg in ionic form and complexed with Dissolved Organic Carbon (DOC). Given all these features, the HR3DHG model can be a useful tool to predict possible effects of climate changes (e.g. increase of temperature, dust inputs, etc.) on mercury dynamics in the environment for very long time intervals.

The paper is organized as follows: a brief overview of the study site is provided in section 2. The description of the HR3DHG model and the model simulation setup are described in Section 3, referring to the Supplement for further details. In Section 4 the obtained results are reported and compared with experimental data. In Section 5 the model and the results are discussed and, finally, conclusions are drawn in Section 6.

2 The study area

The Augusta Bay (Fig.1) is a semi-closed marine area which occupies a surface of about 30 km^2 on the eastern coast of Sicily (southern Italy). The location of one of the most important harbors of the Mediterranean overtime since the early 1960s, the Augusta site also hosts several industrial plants, which have adversely affected the whole area with the diffusion of several priority pollutants. In particular, huge amount of Hg from one of the largest European chlor-alkali plant (Syndial Priolo Gargallo), was discharged into the sea without any treatment until the 1970s, when waste treatment became operational (Bellucci et al., 2012). Although discharge activities were definitively stopped in 2005, the Hg contamination from the chlor-alkali plant remains a critical environmental threat, with extremely high $[Hg]$ in the bottom sediments (Mare, 2008; Sprovieri et al., 2011; Oliveri et al., 2016), significant Hg evasion fluxes from sediments to seawater (Salvagio Manta et al., 2016) and to the atmosphere (Bagnato et al., 2013; Sprovieri, 2015), and evident and recently documented risks for the ecosystem (Tomasello et al., 2012; Bonsignore et al., 2013) and for human health (Bianchi et al., 2006; Bonsignore et al., 2015, 2016). The geographical position, together with its geological and oceanographic features, assign to this area a key role in the Hg inventory at Mediterranean scale. A very narrow shelf develops down to 100-130 m with a mean gradient of about 1.0 degree and a next steep slope characterized by a dense net of canyons dropping to the deep Ionian basin (Budillon et al., 2008). The Augusta Harbor covers a surface of 23.5 km^2 with two main inlets connecting with the open sea: the Scirocco (300 m wide and 13 m deep) and the Levante inlets (400 m wide and 40 m deep). The bottom is mainly flat with an average depth of 15 m, with the exception of a deeper channel about 30 m deep connecting the inner part of the harbor with the Levante inlet. Water circulation inside the port and the exchanges through the inlets are mainly ruled by the wind and tidal forcing. Tidal fluctuations are generally low, with amplitudes ranging between 10 to 20 cm and the winds are generally from Northwest and Northeast with an average speed



around 3 m/s (De Marchis et al., 2014). Water circulation in the outer coastal areas is also mainly affected by wind and tidal forcing and only weakly influenced by the outer baroclinic ocean circulation, which takes place mainly from the shelf break area offshore.

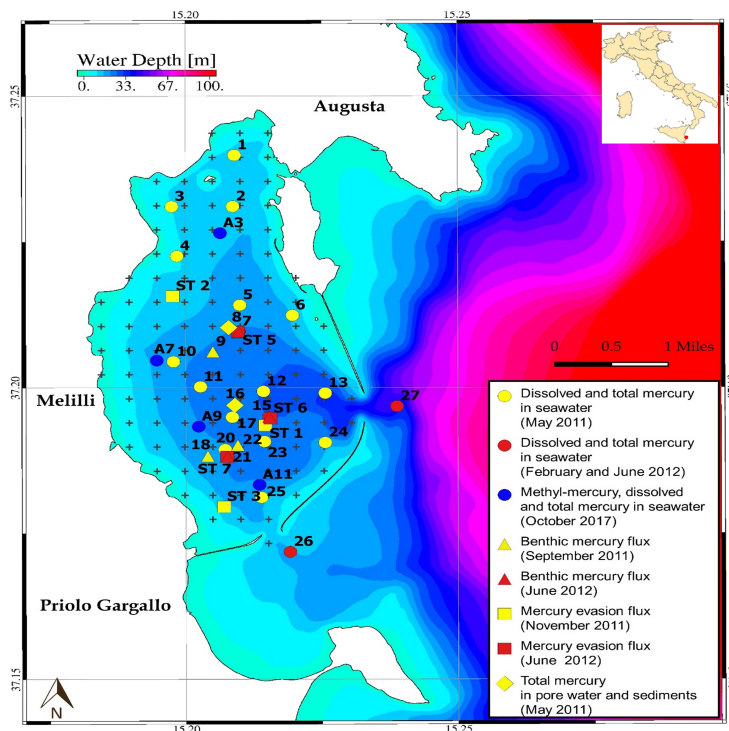


Figure 1. Map of the area under investigation including the Augusta Bay and the eponymous harbor. The sampling sites of each oceanographic survey are indicated with different symbols.

3 Model description

85 The HR3DHG model has been designed and implemented to reconstruct, at high spatio-temporal resolution, the behavior of $[Hg_T]$ and $[Hg_D]$. The model consists of an advection-diffusion-reaction model for the seawater compartment, coupled with a diffusion-reaction sub-model for pore water, in which the dynamics of the sorption/de-sorption of $[Hg_T^{sed}]$ between the solid (sediments) and liquid phase (pore water) is considered.

In the HR3DHG model, the mercury exchange between the abiotic and biotic compartments is also taken into account. For
90 this purpose, the spatio-temporal behavior of eukaryotes abundance is reproduced using the Nutrient-Phytoplankton (NP) model (Dutkiewicz et al., 2009; Morozov et al., 2010; Valenti et al., 2012; Denaro et al., 2013a, c, b; Valenti et al., 2015, 2016a, b, c, 2017), while the amount of Hg absorbed and released by each eukaryotic cell in seawater is calculated by using the



Phytoplankton MERLIN-Expo Model (Ciffroy, 2015; Radomyski and Ciffroy, 2015) (see the Supplement for details). These two modules are coupled with the advection-diffusion-reaction sub-model in order to reproduce the spatio-temporal behavior of the net amount of mercury incorporated by phytoplankton cells in the seawater compartment.

3.1 The advection-diffusion-reaction model for the Hg species in seawater

The dynamics of the $[Hg_D]$ in the Augusta Bay has been reproduced using an advection-diffusion-reaction model (Melaku Canu et al., 2015). Specifically, the model represents the behavior of the three main Hg species in seawater, indicated by $Hg^0(x, y, z, t)$, $Hg^{II}(x, y, z, t)$, and $MeHg(x, y, z, t)$, which denote the concentrations of each Hg species in the position (x, y, z) within the three-dimensional domain at a specific time t , and whose reciprocal interactions are modeled with the reaction terms of the Partial Differential Equations (PDEs). By solving the model equations, we obtain the spatio-temporal distributions of $Hg^0(x, y, z, t)$, $Hg^{II}(x, y, z, t)$, and $MeHg(x, y, z, t)$. The spatial domain is composed by the sum of several sub-domains (regular parallelepipeds), which cover the bathymetric map of the Augusta Bay (Sprovieri et al., 2011). Specifically, z represents the depth of the barycenter of each sub-domain, localized between the surface ($z = 0$) and the bottom ($z = z_b$), while x and y indicate the distance in meters measured from a reference point (Lat. $37^\circ 14.618$ N, Long. $15^\circ 11.069$ E) located at North-West of the town of Augusta.

The model is coded in C++ and adopts a finite volume scheme in explicit form with spatial and temporal discretizations treated separately. The approach followed allows the combination of various types of discretization procedures for solving the diffusion, advection and reaction terms. Specifically, the differential equations are solved by performing centered-in-space differencing for the diffusion terms and first-order upwind-biased differencing for the advection terms.

The model domain is constituted by a mesh of 10 and 18 elements regularly spaced of 454.6 m in both x - and y -direction and with a variable number of vertical layers of 5 m depth in the z -direction. The mesh covers the whole Augusta Harbor and part of the adjacent coastal area. In Fig.1 the model domain is shown along with the location of the open boundaries in correspondence of the two port inlets. A fixed time step of 300 sec has been chosen to satisfy the several stability conditions and constrains associated with the numerical method adopted (Tveito and Winther, 1998). Stability analysis, performed according to previously published methods (Roache, 1998; Tveito and Winther, 1998; Thi et al., 2005), indicates that the convergence of our algorithm is guaranteed.

As initial conditions, we assumed an uniformly distributed concentration of Hg_D and Hg_T , set to 1.9 ng/l corresponding to the experimental detection limit. However, the results appear substantially unaffected by the chosen initial conditions, since the same $[Hg]$ are obtained at nearly-steady state when higher initial Hg concentrations are hypothesized.

The dynamics of the Hg species in seawater is represented through five processes (Zhang et al., 2014; Melaku Canu et al., 2015): i) photochemical and biological redox transformations (reaction terms); ii) methylation/demethylation reactions (reaction terms); iii) movement due to turbulence (diffusion terms); iv) passive drift due to marine currents (advection terms); v) organic particle scavenging/re-mineralization.

The photochemical and biological redox transformations between Hg^0 and Hg^{II} have been described as reaction terms with



a first-order kinetic (Batrakova et al., 2014; Zhang et al., 2014; Melaku Canu et al., 2015). In particular, the rate constants of photochemical redox reactions are directly proportional to the short-wave radiation flux at sea surface then attenuated along the water column due to the dissolved organic carbon (DOC) and suspended particulate matter (*SPM*) (Han et al., 2007; Zhang et al., 2014). At the same time, the rate constants of biological redox reactions are proportional to the organic carbon re-mineralization rate (OCR), which depends on the net primary production at sea surface (NPP), surface chlorophyll concentration and surface atmospheric temperature (Zhang et al., 2014). All data to estimate the rate constants of the redox reactions are derived from remote sensing (see Supplement).

The model includes two reaction terms regulated by first-order kinetics, which describe the photo-demethylation of *MeHg* and the methylation of Hg^{II} , respectively (Monperrus et al., 2007b, a; Whalin et al., 2007). The former is the amount of Hg^{II} produced by the *MeHg* through photochemical reactions. The latter is the amount of *MeHg* obtained by the Hg^{II} through biotic and abiotic pathways in seawater. The rate constants of both reaction terms are fixed according to Melaku Canu et al. 2015 (Melaku Canu et al., 2015).

The PDEs include terms of advection and diffusion for each dimension of the 3D domain. In particular, the diffusion terms reproduce the effects of turbulence on the 3D distribution of Hg_D through horizontal (D_x and D_y) and vertical (D_v) turbulent diffusivities, which are fixed as constant (see Supplement). The horizontal turbulent diffusivity is assumed isotropic in the horizontal water plane ($D_x=D_y$), and calibrated by considering the values obtained in Massel (1999) (Massel, 1999). The vertical turbulent diffusivity is calibrated according with experimental data, which indicate highly stratified water column conditions during the whole year.

The advection terms describe the effects on the *Hg* distributions induced by (i) the horizontal velocity components ($v_x(x, y, z, t)$ and $v_y(x, y, z, t)$) of the marine currents along the x - and y - directions, and (ii) the vertical velocity component ($v_z(x, y, z)$) along the z -direction. The horizontal velocities are calculated using results achieved by applying a hydrodynamic model to the area (Burchard and Petersen, 1999; Umgiesser et al., 2004; Umgiesser, 2009; Umgiesser et al., 2014; Ferrarin et al., 2014; Cucco et al., 2016a, b, 2019) (see Supplement), and change as a function of space and time. The vertical velocity is fixed to zero according to available experimental data.

Moreover, we estimated the dynamics of the dissolved Hg^{II} and *MeHg* species, considering effects due to (i) the adsorption by *SPM* (scavenging process) and (ii) the release by particulate organic matter. The scavenging process for both Hg_D species is regulated by the gradient of mercury concentration along the water column (Zhang et al., 2014)(see Supplement). The amount of mercury released by particulate organic matter is primarily estimated through parameters and variables defined in the NP model and Phytoplankton MERLIN-Expo Model (Valenti et al., 2012; Denaro et al., 2013a, c, b; Valenti et al., 2015, 2016a, b, c, 2017; Radomyski and Ciffroy, 2015)(see Supplement).

Thus, the advection-diffusion-reaction model for the *Hg* species in seawater is defined by the following coupled partial differential equations:

$$\frac{\partial Hg^0}{\partial t} = \frac{\partial}{\partial x} \left[D_x \frac{\partial Hg^0}{\partial x} \right] - \frac{\partial}{\partial x} (v_x Hg^0) + \frac{\partial}{\partial y} \left[D_y \frac{\partial Hg^0}{\partial y} \right] - \frac{\partial}{\partial y} (v_y Hg^0) + \frac{\partial}{\partial z} \left[D_z \frac{\partial Hg^0}{\partial z} \right] - \frac{\partial}{\partial z} (v_z Hg^0) + k_{Ph-de} \cdot MeHg - (k_1 + k_3) \cdot Hg^0 + (k_2 + k_4) \cdot Hg^{II} + S_L^0 \quad (1)$$



$$\frac{\partial Hg^{II}}{\partial t} = + \frac{\partial}{\partial x} \left[D_x \frac{\partial Hg^{II}}{\partial x} \right] - \frac{\partial}{\partial x} (v_x Hg^{II}) + \frac{\partial}{\partial y} \left[D_y \frac{\partial Hg^{II}}{\partial y} \right] - \frac{\partial}{\partial y} (v_y Hg^{II}) + \frac{\partial}{\partial z} \left[D_z \frac{\partial Hg^{II}}{\partial z} \right] - \frac{\partial}{\partial z} (v_z Hg^{II})$$

$$+ (k_1 + k_3) \cdot Hg^0 - (k_2 + k_4) \cdot Hg^{II} - k_{me} \cdot Hg^{II} + S_L^{II} + S_{DOM}^{II} - S_{SPM}^{II} \quad (2)$$

$$\frac{\partial MeHg}{\partial t} = + \frac{\partial}{\partial x} \left[D_x \frac{\partial MeHg}{\partial x} \right] - \frac{\partial}{\partial x} (v_x MeHg) + \frac{\partial}{\partial y} \left[D_y \frac{\partial MeHg}{\partial y} \right] - \frac{\partial}{\partial y} (v_y MeHg) + \frac{\partial}{\partial z} \left[D_z \frac{\partial MeHg}{\partial z} \right]$$

$$- \frac{\partial}{\partial z} (v_z MeHg) - K_{Ph-de} \cdot MeHg + k_{me} \cdot Hg^{II} + S_L^{MM} + S_{DOM}^{MM} - S_{SPM}^{MM} \quad (3)$$

165

Here, k_1 , k_2 , k_3 and k_4 are the rate constants for the photo-oxidation of Hg^0 , the photo-reduction of Hg^{II} , the biological oxidation of Hg^0 and the biological reduction of Hg^{II} , respectively; k_{Ph-de} and k_{me} are the rate constants for the photo-demethylation of $MeHg$ and the methylation of Hg^{II} , respectively; S_L^0 , S_L^{II} and S_L^{MM} are the direct loads for Hg^0 , Hg^{II} and $MeHg$, respectively; S_{DOM}^{II} and S_{DOM}^{MM} are the loads of Hg^{II} and $MeHg$, respectively, released by POM ; S_{SPM}^{II} and S_{SPM}^{MM} are the adsorption rates of SPM for Hg^{II} and $MeHg$, respectively.

170

The advection-diffusion-reaction model is completed by a set of ordinary differential equations (ODEs), which describe the mercury fluxes at the boundaries of Augusta Harbor. Specifically, we take into account for the three mercury species: i) the evasion and the deposition of Hg^0 at the water-atmosphere interface; ii) the lack of Hg^0 diffusion at the water-sediment interface; iii) the deposition of Hg^{II} at the water-atmosphere interface; iv) the lack of deposition of $MeHg$ at the water-atmosphere interface; v) the diffusion of Hg^{II} and $MeHg$ at the water-sediment interface; vi) the exchange of Hg^{II} and $MeHg$ at the seawater-sediment interface due to particulate matter deposition and re-suspension mechanisms; vii) the constant fixed value of $[Hg_D]$ out of Augusta Bay (Ionian Sea); viii) the exchange of the elemental mercury, Hg^{II} and $MeHg$ between the Augusta basin and the Ionian Sea through the two inlets. Since the Augusta Bay is considered as a semi-closed basin, the lateral fluxes at the boundaries of the domain are set to zero except for the two inlets. Here, the lateral fluxes depend on the direction of horizontal velocities, and therefore change as a function of depth and time (see Supplement). The boundary conditions for the three mercury species are defined by the following equations:

175

180

$$\left[D_z \frac{\partial Hg^0}{\partial z} - v_z Hg^0 \right] \Big|_{z=0} = \frac{Hg_{gas-atm} \cdot Pr}{\Delta t} + MTC_{water-atm} \cdot (Hg_{gas-atm} - H \cdot Hg^0|_{z=0}) \quad (4)$$

$$\left[D_x \frac{\partial Hg^0}{\partial x} - v_x Hg^0 \right] = \left[D_y \frac{\partial Hg^0}{\partial y} - v_y Hg^0 \right] = \left[D_z \frac{\partial Hg^0}{\partial z} - v_z Hg^0 \right] \Big|_{z=z_b} = 0 \quad (5)$$

185

$$\left[D_z \frac{\partial Hg^{II}}{\partial z} - v_z Hg^{II} \right] \Big|_{z=0} = \frac{Hg_{atm}^{II} \cdot Pr}{\Delta t}, \quad \left[D_z \frac{\partial MeHg}{\partial z} - v_z MeHg \right] \Big|_{z=0} = \frac{MeHg_{atm} \cdot Pr}{\Delta t} = 0 \quad (6)$$

$$\left[D_z \frac{\partial Hg^{II}}{\partial z} - v_z Hg^{II} \right] \Big|_{z=z_b} = MTC_{sed-water}^{II} \cdot (Hg_{pore-water}^{II} - Hg^{II}|_{z=z_b}) + \phi_{res}^{II} \quad (7)$$



$$190 \quad \left[D_z \frac{\partial MeHg}{\partial z} - v_z MeHg \right]_{z=z_b} = MTC_{sed-water}^{MM} \cdot (MeHg_{pore-water} - MeHg|_{z=z_b}) + \phi_{res}^{MM} \quad (8)$$

$$\left[D_x \frac{\partial Hg^{II}}{\partial x} - v_x Hg^{II} \right] = \left[D_y \frac{\partial Hg^{II}}{\partial y} - v_y Hg^{II} \right] = 0 \quad (9)$$

$$\left[D_x \frac{\partial MeHg}{\partial x} - v_x MeHg \right] = \left[D_y \frac{\partial MeHg}{\partial y} - v_y MeHg \right] = 0 \quad (10)$$

195

$$Hg^0(x_{inlet}, y_{inlet}, z) = Hg_{ext}^0, \quad Hg^{II}(x_{inlet}, y_{inlet}, z) = Hg_{ext}^{II}, \quad MeHg(x_{inlet}, y_{inlet}, z) = MeHg_{ext} \quad (11)$$

where $Hg_{gas-atm}$ is the gaseous elemental mercury (GEM) concentration in atmosphere; Pr is the amount of precipitation; Δt is the exposition time to precipitations; $MTC_{water-atm}$ is the gas phase overall mass transfer coefficient; H is the Henry's law constant; $Hg^0|_{z=0}$ is the $[Hg^0]$ at the sea surface; Hg_{atm}^{II} is the $[Hg^{II}]$ in atmosphere; $MTC_{sed-water}^{II}$ is the mass transfer coefficient for Hg^{II} at the water-sediment interface; $Hg_{pore-water}^{II}$ is the $[Hg^{II}]$ in the pore water of the surface layer (upper 10 cm) of the sediments; $Hg^{II}|_{z=z_b}$ is the dissolved $[Hg^{II}]$ at the deepest layer of the water column ($z = z_b$); ϕ_{res}^{II} is the Hg^{II} flux at the seawater-sediment interface produced by particulate matter deposition and re-suspension processes; $MTC_{sed-water}^{MM}$ is the mass transfer coefficient for $MeHg$ at the water-sediment interface; $MeHg_{pore-water}$ is the $[MeHg]$ in the pore water in the surface layer (upper 10 cm) of the sediments; $MeHg|_{z=z_b}$ is the dissolved $[MeHg]$ in the deepest layer of the water column ($z = z_b$); ϕ_{res}^{MM} is the $MeHg$ flux at the seawater-sediment interface caused by the particulate matter deposition and re-suspension processes; Hg_{ext}^0 , Hg_{ext}^{II} and $MeHg_{ext}$ are the average $[Hg^0]$, $[Hg^{II}]$ and $[MeHg]$, respectively, reported from the Ionian Sea (Horvat et al., 2003; Cossa and Coquery, 2005; Zhang et al., 2014; Melaku Canu et al., 2015). The dynamics of the GEM and Hg^{II} concentrations in the atmosphere ($Hg_{gas-atm}$ and Hg_{atm}^{II}) is reproduced using the experimental data collected in the Augusta Bay between August 2011 and June 2012 (Bagnato et al., 2013), whereas rainfall is derived from the remote sensing (see <http://eosweb.larc.nasa.gov/sse/RETScreen/>). The spatio-temporal dynamics of pore water mercury concentrations ($Hg_{pore-water}^{II}$ and $MeHg_{pore-water}$) at the sediment surface layer are obtained with the diffusion-reaction model for the sediment compartment, while the mass transfer coefficients ($MTC_{sed-water}^{II}$ and $MTC_{sed-water}^{MM}$) at the water-sediment interface are calculated in order to fit the experimental findings and according to previous works (Schulz and Zabel, 2006; Ciffroy, 2015) (see Supplement). The dynamics of the mercury benthic fluxes (ϕ_{res}^{II} and ϕ_{res}^{MM}) caused by particulate matter deposition and re-suspension mechanisms (Neumeier et al., 2008; Ferrarin et al., 2008) is obtained by considering both the spatial distribution of sediment porosity and the spatio-temporal behavior of removed/settled sediment thickness at the seawater-sediment interface. The sediment exchanges at the water-bottom interfase are obtained from the application of the hydrodynamic model, which accounts for sediment transport processes induced by currents (see Supplement).

215 Eqs. (1)-(11) represent the 3D advection-diffusion-reaction model used to describe and reproduce the spatio-temporal dynamics



220 of the three mercury species dissolved in seawater.

The concentrations $[Hg_D]$ and $[Hg_T]$ are calculated as a function of position (x, y, z) and time t , as follows:

$$Hg_D = Hg^0 + Hg^{II} + MeHg \quad (12)$$

$$Hg_T = Hg_D + k_D \cdot SPM \cdot (Hg^{II} + MeHg). \quad (13)$$

Here, k_D is the seawater- SPM partition coefficient for Hg_D (only Hg^{II} and $MeHg$), and SPM is the Suspended Particulate
225 Matter concentration. The partition coefficient k_D has been calibrated to fit experimental data for $[Hg_T]$ and $[Hg_D]$ in the
seawater compartment, thus obtaining a value that is in very good agreement with those reported by Melaku Canu et al. (2015),
Covelli et al. (2008) and Hines et al. (2012), for the Marano-Grado Lagoon (Melaku Canu et al., 2015; Covelli et al., 2008;
Hines et al., 2012). The spatial distribution of SPM was set according to the experimental information collected during the
oceanographic cruise of October 2017.

230 The annual mass balance for the total Hg in the seawater compartment can be estimated, using the boundary conditions given
in Eqs. (4)-(10), according to the following equation (Sprovieri et al., 2011; Salvagio Manta et al., 2016):

$$A + AD + R = O + D + V \quad (14)$$

where A is the input of the Hg_D from anthropogenic activities; AD is the atmospheric mercury deposition; R is the mercury
flux from sediments to seawater due to diffusion processes; O is the net mercury outflow from the Augusta Harbor to the Ionian
235 Sea; D is the amount of mercury recycled in the Augusta Bay (or the net mercury deposition for settling and burial); V is the
GEM evasion from the Augusta Bay to the atmosphere.

By integrating Eqs. (4)-(10), we obtain the terms of the annual mass balance referred to the mercury fluxes exchanged at
the interfaces (AD, R, V), and the net mercury outflow from the Augusta Bay to the Ionian Sea (O), while the input of the
anthropogenic activities (A) is set to zero according to literature sources (Sprovieri et al., 2011; Salvagio Manta et al., 2016).

240 Finally, we estimate the total amount of mercury recycled (D) from the other terms, and compare it with the amount of mercury
recycled by scavenging (S). A simple scheme of the fluxes exchanged in the mercury biogeochemical cycle of the Augusta
Bay is shown in Fig. 2.

3.2 The diffusion-reaction model for Hg species in pore water

The dynamics of $[Hg_D^{sed}]$ and $[Hg_T^{sed}]$ in the Augusta sediments (average thickness of 1.9 m) has been studied using a diffusion-
245 reaction model (see the next Eqs. (16), (17), (18)). In particular, we investigated the behavior of the two mercury species
dissolved in pore water, i.e. Hg^{II} ($Hg_{pore-water}^{II}$) and $MeHg$ ($MeHg_{pore-water}$), which interact with each other directly
through the reaction terms of the two PDEs. Moreover, in the model we took into account the variations of mercury concentra-
tions in pore water due to the slow desorption of the fraction bound to particulate sediments. We describe mercury desorption
using an exponential equation, and assuming this process is regulated by a first-order kinetic.

250 The model provides solutions for the spatio-temporal behavior of mercury concentration, both for the two species dissolved in
pore water, i.e. inorganic mercury ($Hg_{pore-water}^{II}(x', y', z', t)$) and methyl-mercury ($MeHg_{pore-water}(x', y', z', t)$), and the

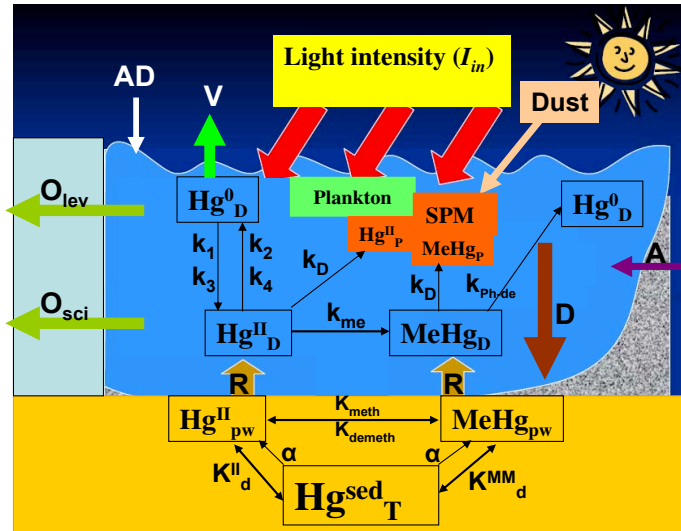


Figure 2. Basic scheme used for implementing the HR3DHG model.

total mercury concentration in the sediments ($Hg_T^{sed}(x', y', z', t)$). Here, the coordinates (x', y', z') indicate the position within the irregular three-dimensional domain of the sediment compartment. Since the surface sediment slope is very low for the whole basin, the domain is approximated as the sum of several sub-domains shaped as regular parallelepipeds, which reproduce the sediment columns in each position (x', y', z') of the Augusta Bay. Specifically, z' represents the depth of the barycenter of each subdomain, localized between the top ($z' = 0$) and the bottom ($z' = 1.9$ m) of the surface sediment layer, while the other coordinates ($x' = x$ and $y' = y$) indicate the distance in meters measured from the same reference point used for the seawater compartment.

In the sediment compartment, the adopted numerical method uses a finite volume scheme in explicit form, where space and time discretization are considered separately. In particular, the PDEs of the model are solved by performing a centered-in-space differencing for the diffusion terms. The sea bottom is discretized in the horizontal plane using the same regular mesh adopted for simulating the dissolved mercury distribution in the seawater compartment (see Fig.1) with 454.6 m regularly spaced elements. In this case, the vertical discretization is constituted by equally spaced layers of 0.2 m depth, with the exception of the interface layer between water and sediment, whose depth is set at 0.1 m. This choice has been made in order to best adapt the 3D grid of the model to the scheme used to interpolate available experimental data. The same fixed time step of 300 sec is adopted to guarantee stability conditions (Roache, 1998; Tveito and Winther, 1998; Thi et al., 2005).

The initial conditions for $[Hg_T^{sed}]$ and $[Hg_D^{sed}]$ are fixed on the basis of experimental findings. As a first step we reproduced the spatial distribution of Hg_T^{sed} at time $t = 0$ by interpolating the experimental data reported in ICRAM (2005) (see Supplement).

We then calculated both $[Hg^{II}]$ and $[MeHg]$ in pore water using the following equations:

$$Hg_{pore-water}^{II}(0) = (1 - k_{MeHg}) \cdot \frac{Hg_T^{sed}(0)}{K_d^{II}}, \quad MeHg_{pore-water}(0) = k_{MeHg} \cdot \frac{Hg_T^{sed}(0)}{K_d^{MM}} \quad (15)$$



where $Hg_T^{sed}(0)$ represents the spatial distribution of $[Hg_T]$ in the sediments at initial time, k_{MeHg} is the fraction of $MeHg$ in the sediments, K_d^{II} is the sediment-pore water distribution coefficient for Hg^{II} , and K_d^{MM} is the sediment-pore water distribution coefficient for $MeHg$.

In pore water, the dynamics of $[Hg^{II}]$ and $[MeHg]$ are modeled by considering three chemical-physical processes (Schulz and Zabel, 2006; Melaku Canu et al., 2015; Oliveri et al., 2016): i) methylation and de-methylation (reaction terms); ii) passive
 275 movement due to the Brownian motion of each chemical species (diffusion terms); iii) desorption of mercury bound to sediment particles (desorption term).

The methylation and de-methylation processes involved in the dynamics of the Hg^{II} and $MeHg$ are considered in the model through reaction terms describing first-order kinetics. The rate constants of these reactions are fixed according to previous
 280 works (Hines et al., 2012; Melaku Canu et al., 2015).

The diffusion terms reproduce the effects of the Brownian motions on the spatial distribution of the $[Hg_D^{sed}]$ in pore water. In particular, the magnitude of the Brownian motions is described by the molecular diffusion coefficients for Hg^{II} ($D_{sed}^{in}(x', y', z')$) and $MeHg$ ($D_{sed}^{or}(x', y', z')$), which change in each position of the domain as a function of porosity and tortuosity (see Supplement). The molecular diffusion coefficients are assumed isotropic in all directions, and are set as constant
 285 functions of time according to previous works (Schulz and Zabel, 2006; Melaku Canu et al., 2015).

The desorption term estimates the increase of $Hg_{pore-water}^{II}$ and $MeHg_{pore-water}$ due to the mercury release from the sediment particles to pore water. The desorption process is regulated by the temporal gradient of $[Hg_T^{sed}]$ ($\partial Hg_T^{sed} / \partial t$), which changes as a function of position and time (see Supplement).

Thus, the module for the sediment compartment is defined by the following coupled partial differential equations:

$$290 \quad \frac{dHg_{pore-water}^{II}}{dt} = +K_{demeth} \cdot MeHg_{pore-water} - K_{meth} \cdot Hg_{pore-water}^{II} + \frac{\partial}{\partial x} \left[D_{sed}^{in} \cdot \frac{\partial Hg_{pore-water}^{II}}{\partial x} \right] + \frac{\partial}{\partial y} \left[D_{sed}^{in} \cdot \frac{\partial Hg_{pore-water}^{II}}{\partial y} \right] + \frac{\partial}{\partial z} \left[D_{sed}^{in} \cdot \frac{\partial Hg_{pore-water}^{II}}{\partial z} \right] - \frac{(1 - k_{MeHg})}{K_d^{II}} \cdot \frac{dHg_T^{sed}}{dt} \quad (16)$$

$$\frac{dMeHg_{pore-water}}{dt} = -K_{demeth} \cdot MeHg_{pore-water} + K_{meth} \cdot Hg_{pore-water}^{II} + \frac{\partial}{\partial x} \left[D_{sed}^{or} \cdot \frac{\partial MeHg_{pore-water}}{\partial x} \right] + \frac{\partial}{\partial y} \left[D_{sed}^{or} \cdot \frac{\partial MeHg_{pore-water}}{\partial y} \right] + \frac{\partial}{\partial z} \left[D_{sed}^{or} \cdot \frac{\partial MeHg_{pore-water}}{\partial z} \right] - \frac{k_{MeHg}}{K_d^{MM}} \cdot \frac{dHg_T^{sed}}{dt} \quad (17)$$

$$295 \quad \frac{dHg_T^{sed}}{dt} = -\alpha \cdot Hg_T^{sed} \Rightarrow Hg_T^{sed}(t) = Hg_T^{sed}(0) \cdot \exp(-\alpha \cdot t) \quad (18)$$

where K_{demeth} is the rate constant for the de-methylation of $MeHg$; K_{meth} is the rate constant for the methylation of Hg^{II} ; α is the desorption rate for the $[Hg_T^{sed}]$ bound to the sediment particles. The spatial distribution of the fraction of methylmercury in the sediments is that obtained by field observations, while the two sediment-pore water distribution coefficients are
 300 calibrated, according to previous work (Oliveri et al., 2016), in order to fit the experimental data. The desorption rate α is fixed to a low value to fit the slow mercury release from the sediment particles to pore water according to experimental observations.



As boundary conditions, we assume a null value of mercury flux at the bottom of the sediment column (1.9 m depth), mainly due to the measured very low porosity, while the vertical gradient of $[Hg_T^{sed}]$ and $[Hg_D^{sed}]$ are set to zero at the water-sediment interface, according to field observations. The mercury concentration in sediments is fixed to zero at the lateral boundaries (x'_b, y'_b) of the 3D domain. The boundary conditions for dissolved and total mercury concentrations in sediments are described by the following equations:

$$\left[D_{sed}^{in} \frac{\partial Hg_{pore-water}^{II}}{\partial z} \right] \Big|_{z'=0} = \left[D_{sed}^{in} \frac{\partial Hg_{pore-water}^{II}}{\partial z} \right] \Big|_{z'=1.9m} = 0 \quad (19)$$

$$\left[D_{sed}^{or} \frac{\partial MeHg_{pore-water}}{\partial z} \right] \Big|_{z'=0} = \left[D_{sed}^{or} \frac{\partial MeHg_{pore-water}}{\partial z} \right] \Big|_{z'=1.9m} = 0 \quad (20)$$

310

$$\left[\frac{\partial Hg_T^{sed}}{\partial z} \right] \Big|_{z'=0} = \left[\frac{\partial Hg_T^{sed}}{\partial z} \right] \Big|_{z'=1.9m} = 0 \quad (21)$$

$$Hg_{pore-water}^{II}|_{(x'_b, y'_b)} = 0, \quad MeHg_{pore-water}|_{(x'_b, y'_b)} = 0, \quad Hg_T^{sed}|_{(x'_b, y'_b)} = 0 \quad (22)$$

Eqs. (16)-(22) represent the three-dimensional diffusion-reaction model used to describe and reproduce the spatio-temporal dynamics of $[Hg^{II}]$ and $[MeHg]$ in pore water, and of $[Hg_T^{sed}]$ in sediments. It is to be noticed that equations (7)-(8), (16)-(17) and (15), which reproduce the spatio-temporal distributions of the mercury concentrations in both compartments (seawater and sediment), strongly depend on the initial condition for the total mercury concentration observed in the sediments.

3.3 Model and simulation setup

In our model, most of the environmental parameters have been set to values experimentally observed in sites contaminated by mercury (Horvat et al., 2003; Schulz and Zabel, 2006; Melaku Canu et al., 2015; Sprovieri et al., 2011; Salvagio Manta et al., 2016; Sunderland et al., 2006; Zhang et al., 2014), while other parameters, among which are those most sensitive for the model, have been calibrated so as to correctly reproduce the experimental data collected during the six oceanographic surveys (Sprovieri et al., 2011; Mare, 2008; Bagnato et al., 2013; Salvagio Manta et al., 2016; Oliveri et al., 2016).

Experimental measurements were carried out during the period between 2005 and 2017 in several stations inside and outside Augusta Harbor (see Fig. 1). Mercury concentration as well as mercury fluxes were measured both in sediments and seawater (see Tables S4-S8, S10 of Supplement). We refer to Bagnato et al. (2013), Salvagio Manta et al. (2016) and Oliveri et al. (2016) for a detailed description of the measured parameters, of the related dynamics and of the analytical methods used (Mare, 2008; Bagnato et al., 2013; Salvagio Manta et al., 2016; Oliveri et al., 2016). These experimental data were used to identify the most sensitive parameters for the model and to compare them with the theoretical results in order to estimate the model accuracy in reproducing Hg dynamics.

330



Concerning the calibration procedure, we first focused on the best values of the parameters for the sediment compartment (i.e. sediment-pore water distribution coefficients, desorption rate and boundary layer thickness above the sediment) in such a way as to optimize the match between theoretical results and experimental observations. More specifically, the sediment-pore water distribution coefficients and the desorption rate were calibrated to guarantee the best theoretical mercury concentration in pore water, whereas the *boundary layer thickness above the sediment* was optimized to better reproduce the spatial distribution of mercury benthic flux observed experimentally. As a second step, we calibrated model parameters for the seawater compartment (i.e. vertical and horizontal diffusivities) in order to better reproduce the spatio-temporal dynamics of the dissolved mercury concentration. In particular, we set the vertical turbulent diffusivity in such a way as to obtain the best match with experimentally observed dissolved mercury concentration along the whole water column. At the same time, the horizontal turbulent diffusivities were optimized to get the best possible match with the observed mercury evasion flux. The calibrated vertical diffusivity was in good agreement with previously reported values (Pacanowski and Philander, 1981; Denman and Gargett, 1983; Peters et al., 1988; Valenti et al., 2015, 2017) under the condition of weakly mixed waters typical of the Augusta Bay. The calibrated horizontal diffusivities were in accordance with the values estimated by other authors (Pacanowski and Philander, 1981; Massel, 1999; Katz et al., 1979) for basins similar in size to those of the Augusta Bay. As a third step, we calibrated the seawater-SPM partition coefficient in order to obtain theoretical distributions of the total mercury concentration in agreement with experimental ones. The partition coefficient obtained was in very good agreement with that previously reported (Hines et al., 2012; Melaku Canu et al., 2015).

In our analysis, no comparison between the calibrated desorption rate and experimental data was possible. However, the other calibrated environmental parameters were in good agreement with those obtained experimentally both in the Augusta Bay and in other sites contaminated by mercury (Melaku Canu et al., 2015; Oliveri et al., 2016; Liu et al., 2012; Cossa and Coquery, 2005; Ciffroy, 2015). The calibrated model has been run for 250 years using as forcing function the environmental data (water currents, wind etc.) provided by hydrodynamic modeling over one year (see Supplement).

4 Results

In the following the simulation results obtained for the seawater and sediment compartments are described and compared with experimental data.

4.1 Mercury in seawater

The spatial distribution of the three mercury species dissolved in seawater is obtained by solving Eqs. (1)-(11), together with the equation system (16)-(22) for the sediment compartment. All environmental parameters and variables used for the seawater compartment are reported in Tables S1-S3 of the Supplement. To reproduce the spatial mercury distributions at near-steady-state, we integrated the model equations over a time interval ($t_{max} > 7 \text{ year}$) long enough to reach an annual decrease of mercury concentration of less than 2 percent. This percentage value progressively declines for longer time intervals down to an annual decrease of 0.12 percent for $t_{max} = 250 \text{ year}$.



The spatio-temporal dynamics of the three mercury species dissolved in seawater is shown in Fig. 3. Here, we observe that the

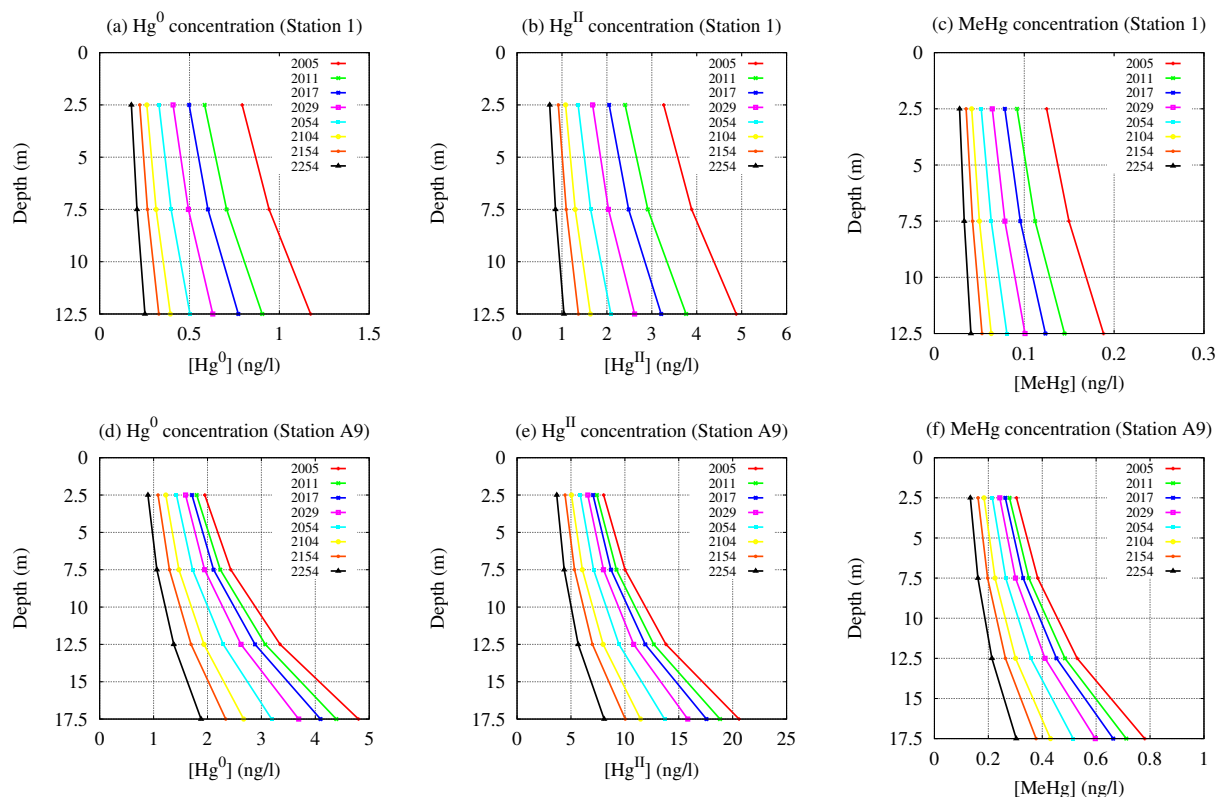


Figure 3. Spatio-temporal evolution of the three mercury species in seawater. Vertical profiles of $[Hg^0]$ (panels a,d), $[Hg^{II}]$ (panels b,e) and $[MeHg]$ (panels c,f) are shown for the sites closest to station 1 (sampling May 2011) and station A9 (sampling October 2017).

concentration ratios among the three mercury species are in excellent agreement with both experimental and theoretical values reported in recent publications (Zhang et al., 2014; Melaku Canu et al., 2015). Moreover, the theoretical results for the vertical profiles of the mercury concentration show a similar shape for the whole simulated period (2005-2254), while the magnitude of the concentrations in the whole water column decreases slowly as a function of time.

In general, the mercury concentration is maximal at the seawater-sediment interface, where the main sources of Hg^{II} and $MeHg$ are localized. However, in some (x,y) sites of the calculation grid (see Fig.1) we observe that the peaks of mercury concentration occur at mid-depth of the water column possibly due to the effects of the velocity field of marine currents and the bathymetric features of Augusta basin.

The dynamics of mercury concentration in seawater is strictly connected with the behavior of the benthic mercury fluxes, which decrease slowly as a function of time due to the slow molecular diffusion process of mercury within the pore waters of the sediments.



375 Comparison of model results and experimental information for $[MeHg]$ indicates a good agreement in stations $A3$ and $A7$, while differences can be observed at the bottom layer of the stations $A9$ and $A11$, where the theoretical concentrations appear overestimated (see Table S4 of the Supplement). This result is probably due to the overestimation of the $MeHg$ benthic fluxes in these two stations.

In our analysis, the spatio-temporal behavior of $[Hg_D]$ is obtained as sum of the three dissolved mercury species. On the other
380 hand, the dynamics of the spatial distribution of the $[Hg_T]$ is obtained using the model prediction for the $[Hg_D]$ and the experimental SPM concentrations. The spatial distributions of $[Hg_D]$ and $[Hg_T]$ are reported for May 2011 in Fig.S1-S4 of the Supplement.

In general, the numerical results for the $[Hg_D]$ are in good agreement with the experimental findings for the four investigated periods (see Table S5 of the Supplement). The comparison for the $[Hg_D]$ indicates small discrepancies and only some specific
385 differences are observed in some of the most contaminated areas, where concentration hot spots are hard to capture given the resolution grid used in the present work.

The model results for $[Hg_T]$ show some discrepancies with experimental data in most of the sites investigated during the first sampling period (May 2011), while in general they evidence a good agreement for the other sampling periods (see Table S6 of the Supplement).

390 The differences (larger than $\sigma = 3.2 \text{ ng/l}$) can be mainly explained by the significant distance between the sampling sites and the model calculation grid nodes (see Fig.1). Additionally, we cannot neglect the role played by the theoretical spatial distribution of the SPM concentration, which could significantly affect the spatio-temporal dynamics of the total mercury concentration in seawater (see Eq. (13)). In particular, the spatial distribution of SPM concentrations, used in the model, probably is not appropriate for the first sampling period investigated (May 2011), while it produces a good agreement for the
395 other three sampling periods.

The theoretical distributions of the benthic mercury fluxes simulated by the model for the two investigated periods (September 2011 and June 2012) are shown in Fig. 4. Here very high benthic Hg^{II} and $MeHg$ fluxes are documented in the south-west sector of Augusta Harbor, where the chlor-alkali plant discharged high amounts of contaminants until the late 1970s. The model reliably reproduces the high benthic mercury fluxes also in the part of the south-east sector close to the inlets of the Augusta
400 Bay, where intensive ship traffic and the relatively high velocity field of the marine currents cause sediment re-suspension and intensive transport of SPM . The benthic mercury fluxes are very low in the coastal zones at the north of the basin, while intermediate values have been calculated in the central part of the bay.

As a whole, the estimated benthic mercury fluxes are in good agreement with the experimental data collected during the two sampling periods (see Table S7 of the Supplement). It should be noted that the model results suggest that the benthic Hg_D
405 fluxes are mainly generated by the diffusion process at the seawater-sediment interface and that the effect of Hg_D release from the re-suspended particulate matter is trivial.

In general, the theoretical distribution of the mercury evasion fluxes is in a very good agreement with the experimental results for the investigated periods (see Table S8 of the Supplement). Only, small discrepancies were observed at station 3 at the end of November 2011, while a larger difference emerged in station 5 during June 2012.

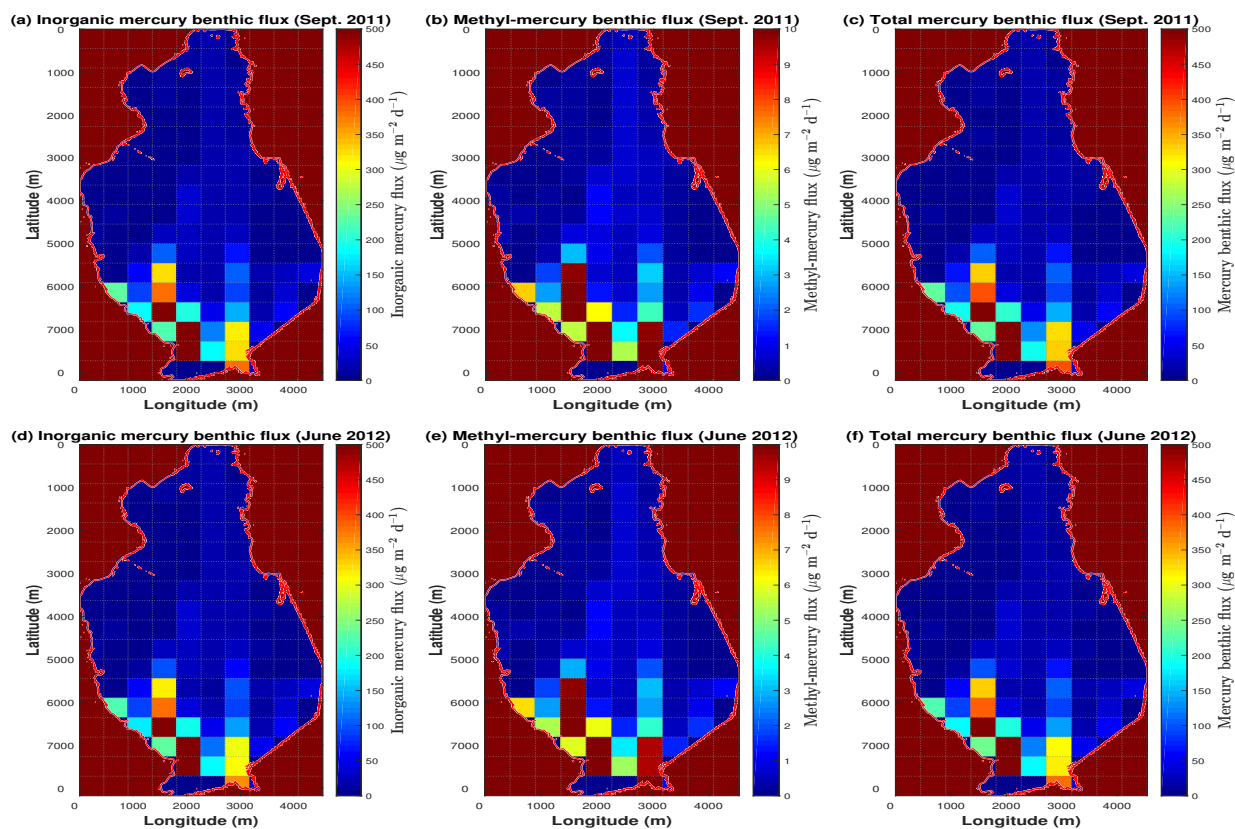


Figure 4. Distribution of Hg^{II} , $MeHg$, and Hg_D fluxes, calculated at the seawater-sediment interface. The maps reproduce the spatial distribution of the benthic flux in the Augusta Bay during the two sampling periods, i.e. 19-21 September 2011 (panels a, b, c) and 23-26 June 2012 (panels d, e, f).

410 The model results for the elemental mercury evasion confirm that a high flux is present in the coastal zones at the south-west of the Augusta Bay, while a reduced evasion flux is observed at the northern sector of the basin (see Fig. 5).

In Fig. 6, we show the temporal behavior of the annual mercury fluxes used for mass balance calculation (see also Table S9 of the Supplement). The results of the annual benthic mercury fluxes (see Fig.6a) show that most of the mercury coming up from sediments is in inorganic form, while the benthic $MeHg$ flux appears to be one to two order of magnitudes lower. The
415 the model results are compared with experimental information reported by Salvagio Manta et al.(2016) (Salvagio Manta et al., 2016) for three different sampling sites and in two different periods (September 2011 and June 2012). The modeled Hg_D benthic fluxes (2.66 kmol y^{-1} for the year 2011 and 2.61 kmol y^{-1} for the year 2012) are significantly larger than those estimated for both sampling periods on the basis of the field observations (1.1 kmol y^{-1} in September 2011 and 1.4 kmol y^{-1} in June 2012) (Salvagio Manta et al., 2016). This probably depends on the limited number of sampling sites available in the
420 experimental work with a consequent extremely coarse capacity to capture reliable estimates of benthic fluxes. Also, the model

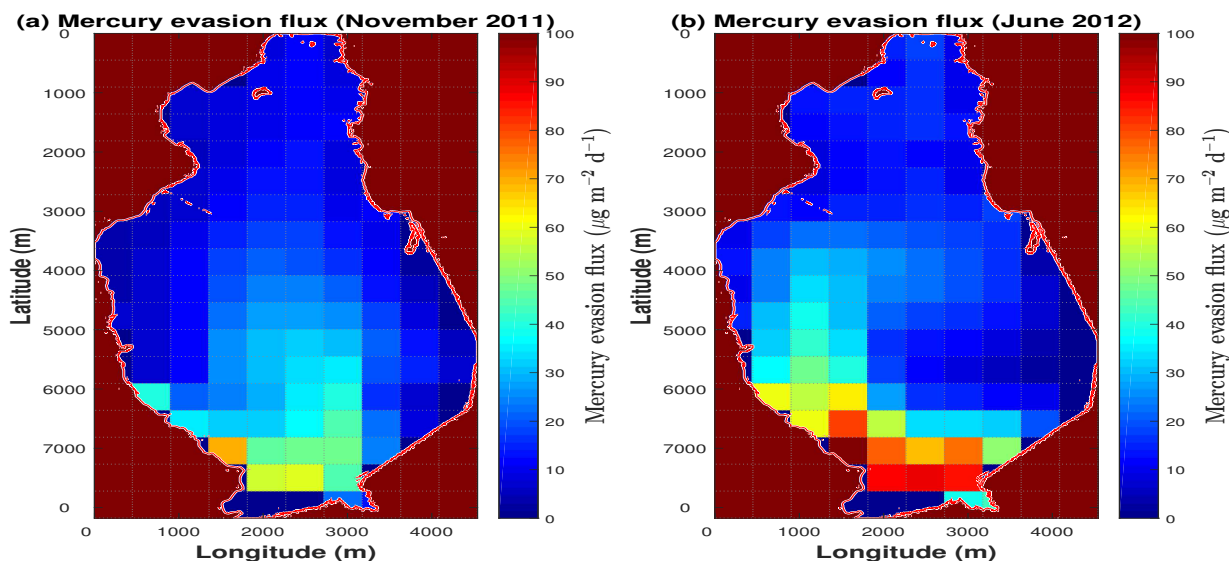


Figure 5. Distribution of Hg^0 flux calculated at the seawater-atmosphere interface. The maps reproduce the spatial distribution of the evasion flux in the Augusta Bay during the two sampling periods, i.e. 29-30 November 2011 (panel a) and 23-25 June 2012 (panel b).

takes into account seasonal variations of mercury concentrations in seawater as well as the effects of marine circulation, thus significantly improving the reliability of the results. Finally, the higher resolution of the grid used in our model guarantees a better estimation of the annual benthic mercury fluxes once the spatio-temporal integration is performed.

The model results for the dynamics of the annual mercury evasion fluxes are shown in Fig.6b. The comparison with experimental findings indicates that the mercury evasion fluxes obtained from the model ($1.78 \cdot 10^{-2} \text{ kmol } y^{-1}$ for the year 2011 and $1.75 \cdot 10^{-2} \text{ kmol } y^{-1}$ for the year 2012) are in very good agreement with those estimated by Salvagio Manta et al. (2016) for each year ($1.70 \cdot 10^{-2} \text{ kmol } y^{-1}$) (Sprovieri, 2015; Salvagio Manta et al., 2016). On the contrary, a significant discrepancy is observed between the annual atmospheric mercury deposition (AD) obtained by our model ($0.17 \cdot 10^{-2} \text{ kmol } y^{-1}$), and that estimated in the experimental work ($0.42 \cdot 10^{-2} \text{ kmol } y^{-1}$) (Salvagio Manta et al., 2016).

The dynamics of the annual net mercury outflow at the Levante and Scirocco inlets is described in Fig.6c. The results encompass both inflow and outflow of the water mass in each inlet for the whole year, and the associated Hg_T contribution (see Supplement). In Fig.6c, we show the annual Hg_T outflow from the Augusta Bay towards the open sea. This has been estimated to be $0.18 \text{ kmol } y^{-1}$ for the year 2012 and appears significantly lower than the $0.51 \text{ kmol } y^{-1}$ calculated by Salvagio Manta et al. (2016) for the same year. Our hypothesis to explain this discrepancy is that the previous study does not consider the dynamics of the $[Hg_T]$ at the inlets (the Hg_T outflow is calculated only on the basis of the mercury concentration measured in February 2012), and that the approach used in the previous paper does not take into account the dynamics of inflow and outflow of the water mass at the two inlets.

The model results for the annual recycled mercury flux are shown in Fig.6d. In this case, values calculated ($2.45 \text{ kmol } y^{-1}$ for

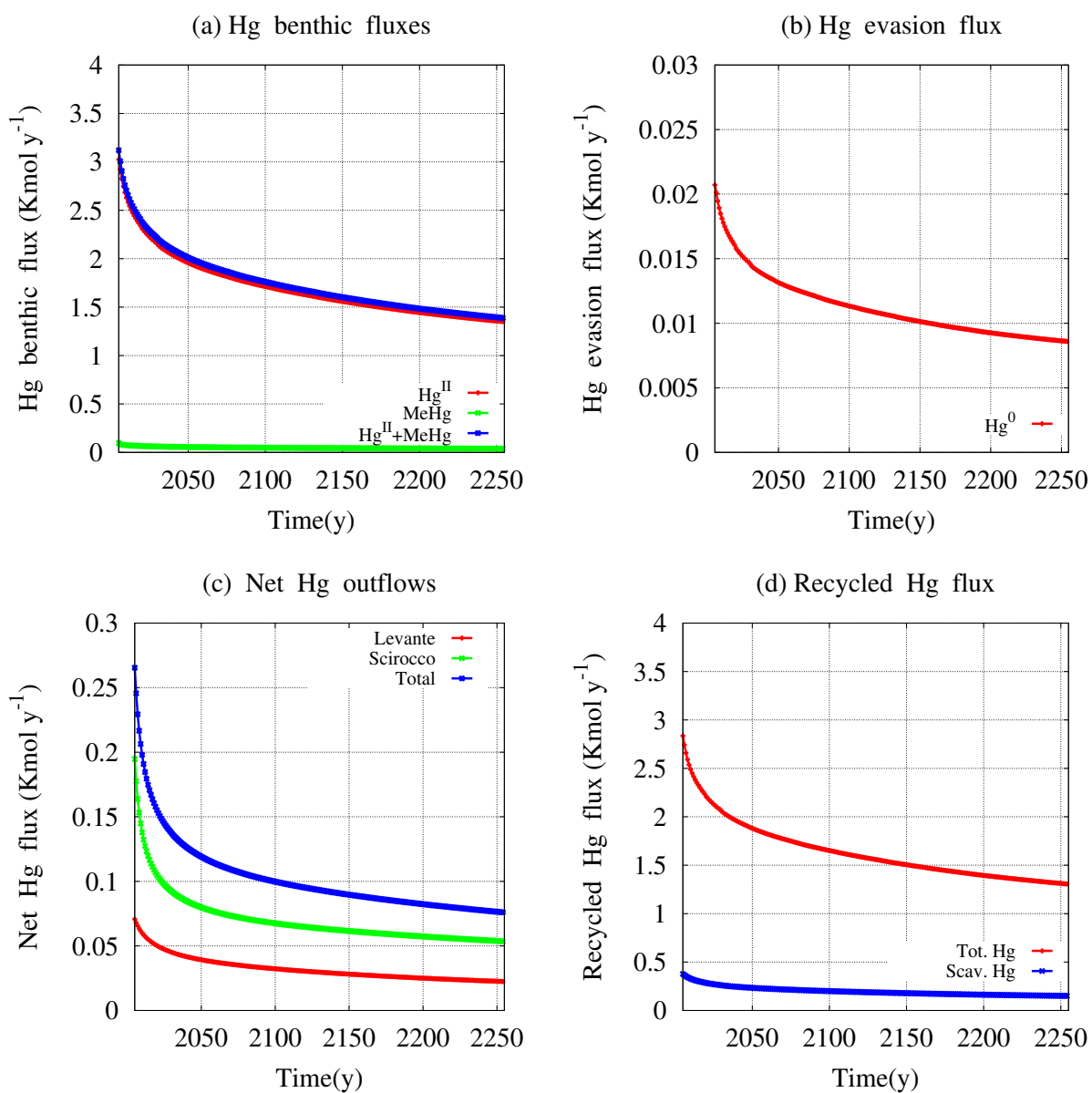


Figure 6. Mercury benthic fluxes (panel a), evasion flux to the atmosphere (panel b), net outflows at the inlets (panel c) and recycling fluxes (panel d).



the year 2011 and 2.41 kmol y^{-1} for the year 2012) are larger and more realistic than those estimated in Salvagio Manta et al. (2016) by simple linear subtraction of the available fluxes in the mass-balance equation (0.84 kmol y^{-1}).

4.2 Mercury in sediments

The spatio-temporal dynamics of $[Hg_T^{sed}]$ in the sediments of Augusta Bay and the mercury concentration of the two species (Hg^{II} and $MeHg$) dissolved in pore water have been obtained by solving Eqs. (16)-(22). All environmental parameters and variables used for the sediment compartment are reported in Tables S1-S2 of the Supplement.

In Fig. 7, the vertical profiles of mercury concentration in the sediments indicate that $[Hg_T^{sed}]$, $[Hg_{pore-water}^{II}]$ and $[MeHg_{pore-water}]$

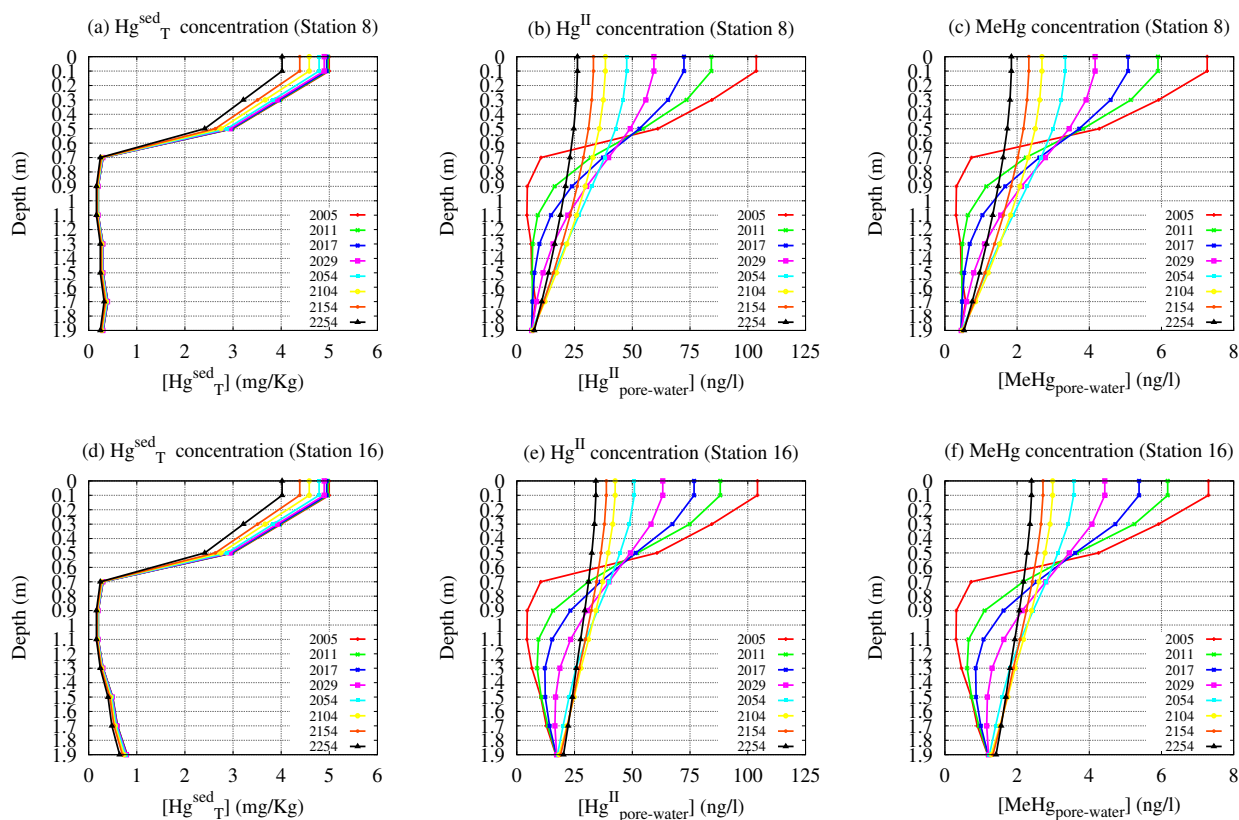


Figure 7. Dynamics of vertical profiles of $[Hg_T^{sed}]$ in sediments (panels a,d), $[Hg^{II}]$ and $[MeHg]$ in pore waters (panels b, c, e and f) at the stations 8 and 16 (sampling May 2011).

always reach their maximum value in the shallower layer of the sediments ($< 0.5 \text{ m}$ of depth). However, the shape of the vertical profiles for $[Hg_{pore-water}^{II}]$ and $[MeHg_{pore-water}]$ in pore water changes as a function of time. Also, the magnitude of the concentration peaks decreases over the whole 3D domain during the period studied. In particular, the pore water mercury



450 concentration assumes a nearly-uniform distribution along the whole sediment column after several years of model simulation, even if the highest mercury concentrations are always observed in the shallowest layer of the sediments. The highest $[Hg_{pore-water}^{II}]$ and $[MeHg_{pore-water}]$ in the sediment surface layer support the high benthic mercury fluxes measured even several years after the chlor-alkali plant closure. Moreover, the results of $[Hg_{pore-water}^{II}]$ and $[MeHg_{pore-water}]$ also indicate that the benthic mercury fluxes will remain elevated until the beginning of 23rd century.

455 Finally, the comparison performed for the $[Hg_D^{sed}]$ in pore water indicates good agreement between the theoretical results and the experimental data (see Table S10 of the Supplement).

5 Discussion

In this work we introduced the innovative HR3DHG biogeochemical model, verified and validated, in all its modules, with the rich database acquired for the Augusta Bay. The model is an advection-diffusion-reaction model (Melaku Canu et al., 2015; Yakushev et al., 2017; Pakhomova et al., 2018; Valenti et al., 2017; Dutkiewicz et al., 2009) that reproduces the spatio-temporal dynamics of the mercury concentration in seawater. The advection-diffusion-reaction model was coupled with: (i) a diffusion-reaction model, which estimates the mercury concentration in the pore waters of the sediment compartment, (ii) the equation which reproduces the mechanism responsible for the desorption of the two mercury species from the solid to the liquid phase of the sediments. This "integrated" model, which allows to give a description of the mercury dynamics in the whole system (seawater, pore water, and particulate phase of the sediment), represents an absolute novelty in the landscape of the mathematical modeling of spatio-temporal dynamics in a biogeochemical context.

This "integrated" model also estimates the total amount of mercury present in biological species which occupy the lowest trophic level of the food chain, i.e. phytoplankton populations. For this purpose, we incorporated the Phytoplankton MERLIN-Expo model (Pickhardt and Fischer, 2007; Radomyski and Ciffroy, 2015) to describe the mechanism of mercury uptake in phytoplankton cells. Moreover, we reproduced the spatio-temporal dynamics of phytoplankton communities in seawater using a Nutrient-Phytoplankton model (Dutkiewicz et al., 2009; Morozov et al., 2010; Valenti et al., 2012; Denaro et al., 2013a, c, b; Valenti et al., 2015, 2016a, b, c, 2017). This "integrated" model, together with the Nutrient-Phytoplankton model and the Phytoplankton MERLIN-Expo model, constitutes a new global biogeochemical (HR3DHG) model describing the mercury dynamics and its effects on the lowest level of the trophic chain.

The HR3DHG model simultaneously provides a high-resolution spatio-temporal dynamics of $[Hg]$ in seawater and sediment, and Hg fluxes at the boundaries of the 3D domain. The former is useful to locate the most polluted areas within the investigated basin. The latter are necessary to obtain the annual mercury mass balance of the basin in the quasi-stationary condition and to predict the mercury outflow towards the open sea, even after a very long time.

480 For comparison, the different approach used in the WASP models and River MERLIN-Expo model allowed neither to reproduce the dynamics of the vertical profiles of mercury concentration in the seawater compartment, nor to obtain the spatio-temporal behavior of mercury concentration in the sediments. Moreover, both the mechanism of the desorption of the total mercury



in sediments and the processes involved in dissolved mercury dynamics in pore water were not taken into account in other advection-diffusion-reaction models, such as the BROM. In general, no forecast about the mercury depletion time in the sediment compartment of Augusta Bay was possible by other models.

485 Finally, the biogeochemical models introduced in previous publications included neither the Nutrient-Phytoplankton model (Dutkiewicz et al., 2009; Morozov et al., 2010; Valenti et al., 2012; Denaro et al., 2013a, c, b; Valenti et al., 2015, 2016a, b, c, 2017) nor the Phytoplankton MERLIN-Expo model for the mercury content in eukaryotes cells (Pickhardt and Fischer, 2007; Radomyski and Ciffroy, 2015).

490 All the aforementioned aspects are therefore an element of novelty in the context of 3D biogeochemical modeling. The HR3DHG model considers the effects of the seasonal changes of the environmental variables on the mercury outflows towards the atmosphere and the open sea, and this also is a new feature in biogeochemical model.

Application of the HR3DHG model to the case study of Augusta Bay provides crucial information for that environment, helping us to revise our view of the mercury dynamics in the highly contaminated coastal marine sites of the Mediterranean sea.

495 Firstly, the mass transfer coefficients at the water-sediment interface are highly sensitive to the *layer thickness above the sediment* and their variation could cause significant changes of mercury benthic fluxes.

Sensitivity analysis performed on the sediment compartment indicates that the spatio-temporal dynamics of the benthic mercury flux strongly depends on the spatial distribution of the sediment porosity and of the initial total mercury concentration in the top-sediments.

500 Sensitivity analysis performed on the environmental parameters and variables used in the seawater compartment indicates that the spatio-temporal dynamics of $[Hg_T]$ and $[Hg_D]$ primarily depends on the velocity field of the marine currents obtained from the hydrodynamic model (Burchard and Petersen, 1999; Umgiesser et al., 2004; Umgiesser, 2009; Umgiesser et al., 2014; Ferrarin et al., 2014; Cucco et al., 2016a, b, 2019), even if the role played by the vertical and horizontal diffusivities (Pacanowski and Philander, 1981; Massel, 1999; Katz et al., 1979; Denman and Gargett, 1983; Peters et al., 1988; Valenti et al., 2015, 2017)

505 cannot be neglected.

The magnitude of the elemental mercury concentration is tightly connected with the values assigned to the rate constants of the photochemical redox reactions, while the role played by the other reaction rates appears negligible for this mercury species.

According to the available experimental data, the theoretical results obtained with the HR3DHG model suggest that the amount of mercury bound to the particulate matter is significantly greater than that dissolved in seawater and pore water. In particular,

510 Hg_D is about 35% of the Hg_T in the seawater compartment, while the amount of mercury dissolved in pore water is negligible with respect to the total amount in the sediments. In general, the concentration of the three mercury species dissolved in seawater decreases slowly as a function of time, whereas their concentration ratios remain approximately constant. Specifically, the mean concentrations of mercury are partitioned as 78% of Hg^{II} , 19% of elemental mercury and 3% of $MeHg$, namely values very similar to those observed experimentally in other contaminated sites (Zhang et al., 2014; Melaku Canu et al., 2015). The

515 same ratio is observed for mercury which outflows from the inlets of Augusta Bay to the open sea. Here, the theoretical results of the HR3DHG model show a progressive decrease in annual mercury outflow from the bay.

On the whole, the mercury dissolved in seawater derives from sediments through the benthic flux of Hg^{II} and $MeHg$. In



particular, these two mercury species are released directly by the sediments, while the elemental mercury is generated by the redox reactions which involve the other two species. The elemental mercury concentration at the water surface contributes to the mercury evasion flux, even if only a small part of elemental mercury in the seawater is released in the atmosphere.

Notably, the theoretical results of the HR3DHG model demonstrate the pivotal role played by the recycling process in the mercury mass balance of the Augusta Bay. Estimates for annual recycled mercury flux indicate that the most part (94%) of the amount of mercury released by sediments remains within the Augusta basin, while the mercury outflows at the boundaries of basin are negligible with respect to the annual benthic mercury fluxes. More specifically, in the quasi-stationary condition, the model results (not shown) indicate that most of the recycled mercury returns to the sediments where is re-buried, and that the amount of mercury absorbed by the phytoplankton, and recycled in seawater, is negligible. In this last respect, it is however important to underscore that even a reduced amount of *MeHg* entering phytoplankton cells can be very dangerous for the health of human beings due to the bio-accumulation processes which occur throughout the food chain.

The dynamics of the particulate matter deposition-resuspension process (Neumeier et al., 2008; Ferrarin et al., 2008) does not significantly modify the spatial distribution of the Hg_T recycled at the surface layer of the sediments. Moreover, the theoretical results show that the recycled mercury flux in the Augusta Bay can only partially be described by the scavenging process of organic particles, which however needs further experimental investigations. In fact, improved knowledge of the scavenging process would be necessary to obtain a better estimation of the Hg_T removed from the water column.

The theoretical results from the HR3DHG model show that, without specific and appropriate recovery actions, the mercury benthic flux could remain high for a very long time, representing a threat for this environment, for its ecosystems and for human health.

Furthermore, climate changes due to the increase in global temperature could significantly influence the dynamics of mercury, with undesirable increases in its concentration and consequent negative effects on the zoobenthos and benthic fishes. The HR3DHG model may represent a useful tool to explore and predict the effects of these possible forthcoming ecological scenarios.

6 Conclusions

A novel biogeochemical integrated model, HR3DHG, has been designed and implemented to reproduce the spatio-temporal dynamics of three species of mercury in the highly contaminated Augusta Bay. The model consistently reproduces the biogeochemical dynamics of mercury fluxes at the boundaries of the 3D domain, which is necessary for an accurate and reliable approximation of the annual mass balance for the whole basin. Direct comparison of model and experimental data suggests a good capacity of HR3DHG to capture the crucial processes dominating the dynamics of *Hg* species in the different marine compartments and at their interfaces, with reliable estimations of benthic fluxes and evasion towards the atmosphere. The model provides robust information on the recycling of the *Hg* species in a confined coastal area and can be considered as a reliable numerical tool to describe high-resolution variability of the most important biogeochemical variables driving *Hg* concentrations. Model results for the Augusta Bay suggest a permanent and relevant long-term (at century scale) mercury benthic



fluxes, associated with negative effects for the biota of the investigated marine ecosystem and with significant health risks. Finally, the HR3DHG model represents a promising tool to explore and predict the effects of climate changes on the mercury dynamics in the marine ecosystems.

Code and data availability. The experimental data used in this study are available and properly referenced along the paper or collected in the tables of the Supplement. The software code files are available on GitHub (<https://doi.org/10.5281/zenodo.3384783>).
555

Author contributions. GD devised the the HR3DHG model; GD, AB and ADG designed the software used to solve numerically the equations of the model; GD and MS jointly wrote the manuscript; DV and BS supported the HR3DHG model development; AB, DV, BS and ADG managed the simulations; DSM and MB performed the Hg data collection; DSM developed the sampling strategy; DSM and MB performed the study of Hg biogeochemistry; MS investigated the Hg biogeochemical dynamics; AC investigated the hydrodynamics in Augusta Bay; AC performed the ocean modelling and generated the code of SHYFEM model; EQ performed the data statistics and mapping. All authors contributed to review the manuscript.
560

Competing interests. The authors declare that they have no conflict of interest.

Acknowledgements. The experimental data used in this study are available and properly referenced along the paper or collected in the tables of the Supplement. We acknowledge the financial support by Ministry of University, Research and Education of Italian Government, Project "Centro Internazionale di Studi Avanzati su Ambiente, ecosistema e Salute umana - CISAS".
565



References

- Bagnato, E., Sprovieri, M., Barra, M., Bitetto, M., Bonsignore, M., Calabrese, S., Di Stefano, V., Oliveri, E., Parello, F., and Mazzola, S.: The sea-air exchange of mercury (Hg) in the marine boundary layer of the Augusta basin (southern Italy): Concentrations and evasion flux, *Chemosphere*, 93, 2024–2032, <https://doi.org/10.1016/j.chemosphere.2013.07.025>, 2013.
- 570 Batrakova, N., Travnikov, O., and Rozovskaya, O.: Chemical and physical transformations of mercury in the ocean: a review, *Ocean Sci.*, 10, 1047–1063, <https://doi.org/https://doi.org/10.5194/os-10-1047-2014>, 2014.
- Bellucci, L. G., Giuliani, S., Romano, S., Albertazzi, S., Mugnai, C., and Frignani, M.: An integrated approach to the assessment of pollutant delivery chronologies to impacted areas: Hg in the Augusta Bay (Italy), *Environ. Sci. Technol.*, 46, 2040–2046, <https://doi.org/10.1021/es203054c>, 2012.
- 575 Bianchi, F., Dardanoni, G., Linzalone, N., and Pierini, A.: Malformazioni congenite nei nati residenti nel Comune di Gela (Sicilia, Italia), *Epidemiol. Prev.*, 30(1), 19–26, 2006.
- Bonsignore, M., Manta, D. S., Oliveri, E., Sprovieri, M., Basilone, G., Bonanno, A., Falco, F., Traina, A., and Mazzola, S.: Mercury in fishes from Augusta Bay (southern Italy): risk assessment and health implication, *Food Chem. Toxicol.*, 56, 184–194, <https://doi.org/10.1016/j.fct.2013.02.025>, 2013.
- 580 Bonsignore, M., Tamburrino, S., Oliveri, E., Marchetti, A., Durante, C., Berni, A., Quinci, E., and Sprovieri, M.: Tracing mercury pathways in Augusta Bay (southern Italy) by total concentration and isotope determination, *Environ. Pollut.*, 205, 178–185, <https://doi.org/10.1016/j.envpol.2015.05.033>, 2015.
- Bonsignore, M., Andolfi, N., Barra, M., Madeddu, M., Tisano, F., Ingallinella, V., Castorina, M., and Sprovieri, M.: Assessment of mercury exposure in human populations: a status report from Augusta Bay (southern Italy), *Environ. Res. Spec. Issue Hum. Biomonitoring*, 150, 592–599, <https://doi.org/10.1016/j.envres.2016.01.016>, 2016.
- 585 Budillon, F., Ferraro, L., Hopkins, T. S., Iorio, M., Lubritto, C., Sprovieri, M., Bellonia, A., Marzaioli, F., and Tonielli, R.: Effects of intense anthropogenic settlement of coastal areas on seabed and sedimentary systems: a case study from the Augusta Bay (southern Italy), *Rend. Online Soc. Geol. Italy*, 3, 142–143, 2008.
- Burchard, H. and Petersen, O.: Models of turbulence in the marine environment. A comparative study of two-equation turbulence models, *J. Mar. Syst.*, 21(1–4), 23–53, [https://doi.org/10.1016/S0924-7963\(99\)00004-4](https://doi.org/10.1016/S0924-7963(99)00004-4), 1999.
- 590 Ciffroy, P.: The River MERLIN-Expo model, Fun Project 4 - Seventh Framework Programme, 2015.
- Cossa, D. and Coquery, M.: The Handbook of Environmental Chemistry, Vol. 5, Part K (2005): 177–208. The Mediterranean Mercury Anomaly, a Geochemical or a Biological Issue, Springer-Verlag Berlin Heidelberg, 2005.
- Covelli, S., Faganeli, J., De Vittor, C., Predonzani, S., Acquavita, A., and Horvat, M.: Benthic fluxes of mercury species in a lagoon environment (Grado Lagoon, Northern Adriatic Sea, Italy), *Appl. Geochem.*, 23, 529–546, <https://doi.org/10.1016/j.apgeochem.2007.12.011>, 2008.
- 595 Cucco, A., Quattrocchi, G., Olita, A., Fazioli, L., Ribotti, A., Sinerchia, M., Tedesco, C., and Sorgente, R.: Hydrodynamic modeling of coastal seas: the role of tidal dynamics in the Messina Strait, Western Mediterranean Sea, *Nat. Hazard Earth Sys.*, 16, 1553–1569, <https://doi.org/10.5194/nhess-16-1553-2016>, 2016a.
- 600 Cucco, A., Quattrocchi, G., Satta, A., Antognarelli, F., De Biasio, F., Cadau, E., Umgiesser, G., and Zecchetto, S.: Predictability of wind-induced sea surface transport in coastal areas, *J. Geophys. Res. Oceans*, 121(8), 5847–5871, <https://doi.org/https://doi.org/10.1002/2016JC011643>, 2016b.



- Cucco, A., Quattrocchi, G., and Zecchetto, S.: The role of temporal resolution in modeling the wind induced sea surface transport in coastal seas, *J. Mar. Syst.*, 193, 46–58, <https://doi.org/https://doi.org/10.1016/j.jmarsys.2019.01.004>, 2019.
- 605 De Marchis, M., Freni, G., and Napoli, E.: Three-dimensional numerical simulations on wind- and tide-induced currents: The case of Augusta Harbour (Italy), *Comput. Geosci.*, 72, 65–75, 2014.
- Denaro, G., Valenti, D., La Cognata, A., Spagnolo, B., Bonanno, A., Basilone, G., Mazzola, S., Zgozi, S., Aronica, S., and Brunet, C.: Spatio-temporal behaviour of the deep chlorophyll maximum in Mediterranean Sea: Development of a stochastic model for picophytoplankton dynamics, *Ecol. Complex.*, 13, 21–34, <https://doi.org/10.1016/j.ecocom.2012.10.002>, 2013a.
- 610 Denaro, G., Valenti, D., Spagnolo, B., Basilone, G., Mazzola, S., Zgozi, S., Aronica, S., and Bonanno, A.: Dynamics of two picophytoplankton groups in Mediterranean Sea: Analysis of the Deep Chlorophyll Maximum by a stochastic advection-reaction-diffusion model, *PLoS ONE*, 8(6), e66765, <https://doi.org/10.1371/journal.pone.0066765>, 2013b.
- Denaro, G., Valenti, D., Spagnolo, B., Bonanno, A., Basilone, G., Mazzola, S., Zgozi, S., and Aronica, S.: Stochastic dynamics of two picophytoplankton populations in a real marine ecosystem, *Acta Phys. Pol. B*, 44, 977–990, <https://doi.org/10.5506/APhysPolB.44.977>,
615 2013c.
- Denman, K. L. and Gargett, A. E.: Time and space scales of vertical mixing and advection of phytoplankton in the upper ocean, *Limnol. Oceanogr.*, 28, 801–815, <https://doi.org/https://doi.org/10.4319/lo.1983.28.5.0801>, 1983.
- Driscoll, C. T., Mason, R. P., Chan, H. M., Jacob, D. J., and Pirrone, N.: Mercury as a Global Pollutant: Sources, Pathways, and Effects, *Environ. Sci. Technol.*, 47, 4967–4983, <https://doi.org/10.1021/es305071v>, 2013.
- 620 Dutkiewicz, S., Follows, M. J., and Bragg, J. G.: Modeling the coupling of ocean ecology and biogeochemistry., *Global Biogeochem. Cycles*, p. GB4017, <https://doi.org/https://doi.org/10.1029/2008GB003405>, 2009.
- Ferrarin, C., Umgiesser, G., Cucco, A., Hsu, T. W., Roland, A., and Amos, C. L.: Development and validation of a finite element morphological model for shallow water basins, *Coast. Eng.*, 55, 716–731, <https://doi.org/10.1016/j.coastaleng.2008.02.016>, 2008.
- Ferrarin, C., Bajo, M., Bellafiore, D., Cucco, A., De Pascalis, F., and Ghezzi, M.: Toward homogenization of Mediterranean lagoons and
625 their loss of hydrodiversity, *Geophys. Res. Lett.*, 41(16), 5935–5941, <https://doi.org/https://doi.org/10.1002/2014GL060843>, 2014.
- Fiasconaro, A., Valenti, D., and Spagnolo, B.: Nonmonotonic Behaviour of Spatiotemporal Pattern Formation in a Noisy Lotka-Volterra System, *Acta Phys. Pol. B*, 35, 1491–1500, 2004.
- Han, S., Lehman, R. D., Choe, K. Y., and Gill, A.: Chemical and physical speciation of mercury in Offatts Bayou: A seasonally anoxic bayou in Galveston Bay, *Limnol. Oceanogr.*, 52(4), 1380–1392, <https://doi.org/https://doi.org/10.4319/lo.2007.52.4.1380>, 2007.
- 630 Hines, M. E., Potrait, E. N., Covelli, S., Faganeli, J., Emili, A., Zizek, E., and Horvat, M.: Mercury methylation and demethylation in Hg-contaminated lagoon sediments (Marano and Grado Lagoon, Italy), *Estuar. Coast. Shelf Sci.*, 113, 85–95, <https://doi.org/10.1016/j.ecss.2011.12.021>, 2012.
- Horvat, M., Kotnik, J., Logar, M., Fajon, V., Zvoranic, T., and Pirrone, N.: Speciation of mercury in surface and deep-sea waters in the Mediterranean Sea, *Atmospheric Environ.*, 37(1), S93–S108, [https://doi.org/10.1016/S1352-2310\(03\)00249-8](https://doi.org/10.1016/S1352-2310(03)00249-8), 2003.
- 635 Katz, E. J., Bruce, J. G., and Petrie, B. D.: Salt and mass flux in the Atlantic Equatorial Undercurrent, *Deep-Sea Res.*, 26, 139–160, 1979.
- La Barbera, A. and Spagnolo, B.: Spatio-Temporal Patterns in Population Dynamics, *Physica A*, 314, 120–124, [https://doi.org/10.1016/S0378-4371\(02\)01173-1](https://doi.org/10.1016/S0378-4371(02)01173-1), 2002.
- Lee, C. S. and Fischer, N. S.: Bioaccumulation of methylmercury in a marine copepod, *Environ Toxicol Chem.*, 36(5), 1287–1293, <https://doi.org/10.1002/etc.3660>, 2017.



- 640 Liu, G., Cai, J., and O'Driscoll, N.: Environmental Chemistry and Toxicology of Mercury, John Wiley and Sons, Inc., Hoboken, New Jersey, 2012.
- Mare, I. I. C. P. L. R. S. E. T. A. A.: Progetto preliminare di bonifica dei fondali della rada di Augusta nel sito di interesse nazionale di Priolo e Elaborazione definitiva, BoI-Pr-SI-PR-Rada di Augusta-03.22, 2008.
- Massel, S. R.: Fluid Mechanics for Marine Ecologists, Springer-Verlag, Berlin Heidelberg, 1999.
- 645 Melaku Canu, D., Rosati, G., Solidoro, C., Heimbürger, L., and Acquavita, A.: A comprehensive assessment of the mercury budget in the Marano-Grado Lagoon (Adriatic Sea) using a combined observational modeling approach, *Mar. Chem.*, 177, 742–752, <https://doi.org/10.1016/j.marchem.2015.10.013>, 2015.
- Monperrus, M., Tessier, E., Amouroux, D., Leynaert, A., Huonnic, P., and Donard, O. F. X.: Mercury methylation, demethylation and reduction rates in coastal and marine surface waters of the Mediterranean Sea, *Mar. Chem.*, 107, 49–63, <https://doi.org/10.1016/j.marchem.2007.01.018>, 2007a.
- 650 Monperrus, M., Tessier, E., Point, D., Vidimova, K., Amouroux, D., Guyoneaud, R., Leynaert, A., Grall, J., Chauvaud, L., Thouzeau, G., and Donard, O. F. X.: The biogeochemistry of mercury at the sediment-water interface in the Thau Lagoon. 2. Evaluation of mercury methylation potential in both surface sediment and the column, *Estuar. Coast. Shelf Sci.*, 72, 485–486, <https://doi.org/https://doi.org/10.1016/j.ecss.2006.11.014>, 2007b.
- 655 Morozov, A., Arashkevich, E., Nikishina, A., and Solovyev, K.: Nutrient-rich plankton communities stabilized via predator-prey interactions: revisiting the role of vertical heterogeneity, *Math. Med. Biol.*, 28(2), 185–215, <https://doi.org/10.1093/imammb/dqq010>, 2010.
- Neumeier, U., Ferrarin, C., Amos, C. L., Umgieser, G., and Li, M. Z.: Sedtrans05: An improved sediment-transport model for continental shelves and coastal waters with a new algorithm for cohesive sediments, *Comput. Geosci.*, 34, 1223–1242, <https://doi.org/10.1016/j.cageo.2008.02.007>, 2008.
- 660 Oliveri, E., Manta, D. S., Bonsignore, M., Cappello, S., Tranchida, G., Bagnato, E., Sabatino, N., Santisi, S., and Sprovieri, M.: Mobility of mercury in contaminated marine sediments: Biogeochemical pathways, *Mar. Chem.*, 186, 1–10, <https://doi.org/10.1016/j.marchem.2016.07.002>, 2016.
- Pacanowski, R. and Philander, S. G. H.: Parameterization of Vertical Mixing in Numerical Models of Tropical Oceans, *J. Phys. Oceanogr.*, 11, 1443–1451, [https://doi.org/10.1175/1520-0485\(1981\)011<1443:POVMIN>2.0.CO;2](https://doi.org/10.1175/1520-0485(1981)011<1443:POVMIN>2.0.CO;2), 1981.
- 665 Pakhomova, S. V., Yakushev, E. V., Protsenko, E. A., Rigaud, S., Cossa, D., Knoery, J., Couture, R. M., Radakovitch, O., Yakubov, S. K., Krzeminska, D., and Newton, A.: Modeling the Influence of Eutrophication and Redox Conditions on Mercury Cycling at the Sediment-Water Interface in the Berre Lagoon, *Front. Mar. Sci.*, 5, 291, <https://doi.org/10.3389/fmars.2018.00291>, 2018.
- Peters, H., Gregg, M. C., and Toole, J. M.: On the Parameterization of Equatorial Turbulence, *J. Geophys. Res.*, 93, 1199–1218, <https://doi.org/https://doi.org/10.1029/JC093iC02p01199>, 1988.
- 670 Pickhardt, P. C. and Fischer, N. S.: Accumulation of Inorganic and Methylmercury by Freshwater Phytoplankton in Two Contrasting Water Bodies, *Environ. Sci. Technol.*, 41, 125–131, <https://doi.org/10.1021/es060966w>, 2007.
- Radomyski, A. and Ciffroy, P.: The Phytoplankton MERLIN-Expo model, Fun Project 4 - Seventh Framework Programme, 2015.
- Roache, P. J.: Fundamentals of Computational Fluid Dynamics, Hermosa Publishers, Albuquerque, New Mexico, 1998.
- Salvagio Manta, D., Bonsignore, M., Oliveri, E., Barra, M., Tranchida, G., Giaramita, L., Mazzola, S., and Sprovieri, M.: Fluxes and the mass balance of mercury in Augusta Bay (Sicily, southern Italy), *Estuar. Coast. Shelf Sci.*, 181, 134–143, <https://doi.org/10.1016/j.ecss.2016.08.013>, 2016.
- Schulz, H. D. and Zabel, M.: Marine Geochemistry, Springer - Verlag Berlin Heidelberg, 2006.



- Sprovieri, M.: Inquinamento ambientale e salute umana, il caso studio della Rada di Augusta, CNR Edizioni, P. Aldo Moro, 7, I-00185 Roma, Italia, 2015.
- 680 Sprovieri, M., Oliveri, E., Di Leonardo, R., Romano, E., Ausili, A., Gabellini, M., Barra, M., Tranchida, G., Bellanca, A., Neri, R., Budillon, F., Saggiomo, R., Mazzola, S., and Saggiomo, V.: The key role played by the Augusta basin (southern Italy) in the mercury contamination of the Mediterranean Sea, *J. Environ. Monit.*, 13, 1753–1760, <https://doi.org/10.1039/C0EM00793E>, 2011.
- Sunderland, E. M., Gobas, F. A. P. C., Branfireum, B. A., and Heyes, A.: Environmental controls on the speciation and distribution of mercury in coastal sediments, *Mar. Chem.*, 102, 111–123, <https://doi.org/10.1016/j.marchem.2005.09.019>, 2006.
- 685 Thi, N. N. P., Huisman, J., and Sommeijer, B. P.: Simulation of three-dimensional phytoplankton dynamics: competition in light-limited environments, *J. Comput. Appl. Math.*, 174, 57–77, <https://doi.org/10.1016/j.cam.2004.03.023>, 2005.
- Tomasello, B., Copat, C., Pulvirenti, V., Ferrito, V., Ferrante, M., Renis, M., Sciacca, S., and Tigano, C.: Biochemical and bioaccumulation approaches for investigating marine pollution using Mediterranean rainbow wrasse, *Coris julis* (Linnaeus 1798), *Ecotoxicol. Environ. Safe.*, 86, 168–175, <https://doi.org/10.1016/j.ecoenv.2012.09.012>, 2012.
- 690 Tveito, A. and Winther, R.: *Introduction to Partial Differential Equations: A Computational Approach*, Springer-Verlag, New York, 1998.
- Umgiesser, G.: SHYFEM. Finite Element Model for Coastal Seas. User Manual, The SHYFEM Group, Georg Umgiesser, ISMAR-CNR, Venezia, Italy, 2009.
- Umgiesser, G., Canu, D. M., Cucco, A., and Solidoro, C.: A finite element model for the Venice Lagoon. Development, set up, calibration and validation, *J. Mar. Syst.*, 51, 123–145, <https://doi.org/10.1016/j.jmarsys.2004.05.009>, 2004.
- 695 Umgiesser, G., Ferrarin, C., Cucco, A., De Pascalis, F., Bellafiore, D., Ghezzi, M., and Bajo, M.: Comparative hydrodynamics of 10 Mediterranean lagoons by means of numerical modeling, *J. Geophys. Res. Oceans*, 119(4), 2212–2226, <https://doi.org/https://doi.org/10.1002/2013JC009512>, 2014.
- Valenti, D., Fiasconaro, A., and Spagnolo, B.: Pattern formation and spatial correlation induced by the noise in two competing species, *Acta Phys. Pol. B*, 35, 1481–1489, 2004.
- 700 Valenti, D., Tranchina, L., Cosentino, C., Brai, M., Caruso, A., and Spagnolo, B.: Environmental Metal Pollution Considered as Noise: Effects on the Spatial Distribution of Benthic Foraminifera in two Coastal Marine Areas of Sicily (Southern Italy), *Ecol. Model.*, 213, 449–462, <https://doi.org/10.1016/j.ecolmodel.2008.01.023>, 2008.
- Valenti, D., Denaro, G., La Cognata, A., Spagnolo, B., Bonanno, A., Mazzola, S., Zgozi, S., and Aronica, S.: Picophytoplankton dynamics in noisy marine environment, *Acta Phys. Pol. B*, 43, 1227–1240, <https://doi.org/10.5506/APhysPolB.43.1227>, 2012.
- 705 Valenti, D., Denaro, G., Spagnolo, B., Conversano, F., and Brunet, C.: How diffusivity, thermocline and incident light intensity modulate the dynamics of deep chlorophyll maximum in Tyrrhenian Sea, *PLoS ONE*, 10(1), e0115468, <https://doi.org/https://doi.org/10.1371/journal.pone.0115468>, 2015.
- Valenti, D., Denaro, G., Conversano, F., Brunet, C., Bonanno, A., Basilone, G., Mazzola, S., and Spagnolo, B.: The role of noise on the steady state distributions of phytoplankton populations, *J. Stat. Mech.*, p. 054044, <https://doi.org/10.1088/1742-5468/2016/05/054044>, 2016a.
- 710 Valenti, D., Denaro, G., Spagnolo, B., Mazzola, S., Basilone, G., Conversano, F., Brunet, C., and Bonanno, A.: Stochastic models for phytoplankton dynamics in Mediterranean Sea, *Ecol. Complex.*, 27, 84–103, <https://doi.org/10.1016/j.ecocom.2015.06.001>, 2016b.
- Valenti, D., Giuffrida, A., Denaro, G., Pizzolato, N., Curcio, L., Mazzola, S., Basilone, G., Bonanno, A., and Spagnolo, B.: Noise Induced Phenomena in the Dynamics of Two Competing Species, *Math. Model. Nat. Phenom.*, 11(5), 158–174, <https://doi.org/https://doi.org/10.1051/mmnp/201611510>, 2016c.



- 715 Valenti, D., Denaro, G., Ferreri, R., Genovese, S., Aronica, S., Mazzola, S., Bonanno, A., Basilone, G., and Spagnolo, B.: Spatio-temporal dynamics of a planktonic system and chlorophyll distribution in a 2D spatial domain: matching model and data, *Sci. Rep.*, 7, 220, <https://doi.org/https://doi.org/10.1051/mmnp/201611510>, 2017.
- Whalin, L., Kim, E., and Mason, R.: Factors influencing the oxidation, reduction, methylation and demethylation of mercury species in coastal waters, *Mar. Chem.*, 107, 278–294, <https://doi.org/10.1016/j.marchem.2007.04.002>, 2007.
- 720 Williams, J. J., Dutton, J., Chen, C. Y., and Fischer, N. S.: Metal (As, Cd, Hg, and CH_3Hg) bioaccumulation from water and food by the benthic amphipod *Leptocheirus Plumulosus*, *Environ. Toxicol. Chem.*, 29(8), 1755–1761, <https://doi.org/10.1002/etc.207>, 2010.
- Yakushev, E. V., Protsenko, E. A., Bruggeman, J., Wallhead, P., Pakhomova, S. V., Yakubov, S. K., Bellerby, R. G. J., and Couture, R. M.: Bottom RedOx Model (BROM v.1.1): a coupled benthic-pelagic model for simulation of water and sediment biogeochemistry, *Geosci. Model Dev.*, 10, 453–482, <https://doi.org/10.5194/gmd-10-453-2017>, 2017.
- 725 Zhang, Y., Jaeglé, L., and Thompson, L.: Natural biogeochemical cycle of mercury in a global three-dimensional ocean tracer model, *Global Biogeochem. Cy.*, 28, GB004 814, <https://doi.org/10.1002/2014GB004814>, 2014.